NJ

DISCRETE LEVELS OF METEOR BEGINNING HEIGHT

Z. CEPLECHA

N68-32720

FACILITY FORM 602

(ACCESSION NUMBER) (THRU)

60 1

(PAGES) (CODE)

CR-96295 30

(NASA CR OR TMX OR AD NUMBER) (CATEGORY)

GPO PRICE $ _____

CFSTI PRICE(S) $ _____

Hard copy (HC) 3.00

Microfiche (MF) .65

ff 653 July 65

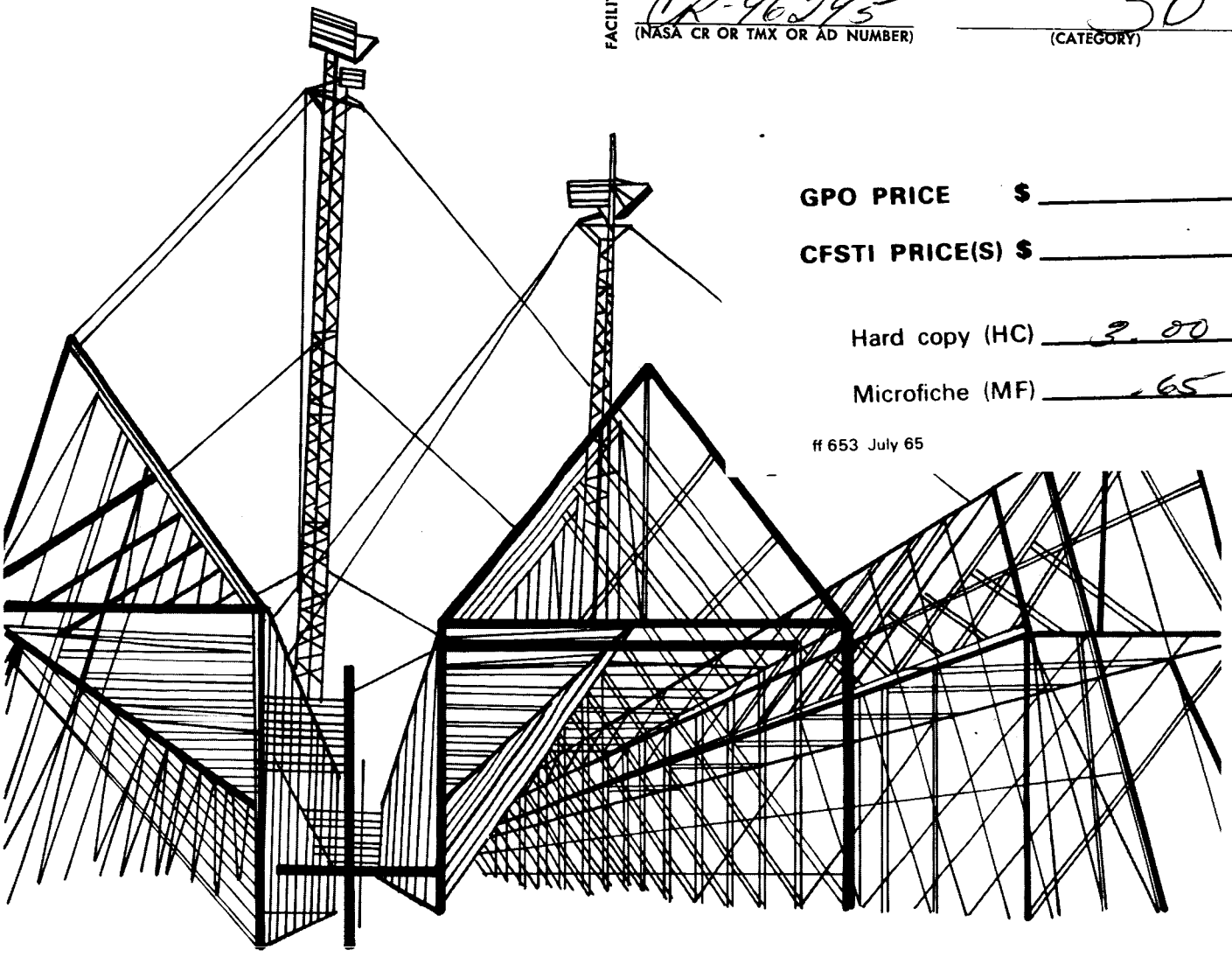

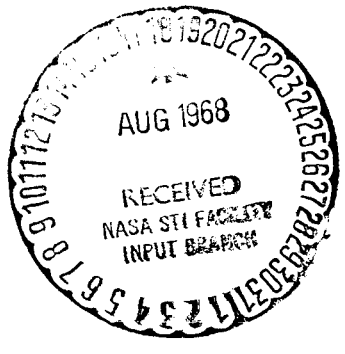

Smithsonian Astrophysical Observatory
SPECIAL REPORT 279

Research in Space Science
SAO Special Report No. 279

DISCRETE LEVELS OF METEOR BEGINNING HEIGHT

Zdeněk Ceplecha

June 7, 1968

Smithsonian Institution
Astrophysical Observatory
Cambridge, Massachusetts 02138

804-41

PRECEDING PAGE BLANK NOT FILMED.

TABLE OF CONTENTS

LIST OF ILLUSTRATIONS

LIST OF ILLUSTRATIONS (Cont.)

ABSTRACT

Discrete levels of meteor beginning height are studied in detail, mainly by means of h_B-v_∞ plots. A summary of the observational evidence is presented. Among the interpretations of these discrete levels, composition and fragmentation seem to be the most important.

RÉSUMÉ

Les niveaux discrets de l'altitude d'apparition de météore ont été étudiés en détail, principalement à l'aide de représentations graphiques de h_B en fonction de v_∞. Un résumé des faits observés est présenté. La composition et la fragmentation semblent être les plus importantes de toutes les interprétations de ces niveaux discrets.

КОНСПЕКТ

Произведено подробное изучение дискретных уровней высоты появления метеора, главным образом с помощью h_B-v_∞ графиков. Представляется краткое изложение данных наблюдений. Среди различных об'яснений этих дискретных уровней, состав и дробление кажутся наиболее важными.

DISCRETE LEVELS OF METEOR BEGINNING HEIGHT

Z. Ceplecha

1. INTRODUCTION

Two distinct levels of beginning height of meteors were first independently reported in 1958 (Ceplecha 1958; Jacchia, 1958, 1960). An extensive study of the problem was published (Ceplecha, 1967), in which the k_B parameter and orbital elements were used. The definition of the k_B parameter is very simple ($k_B = \log \rho_B + 2.5 \log v_\infty - 0.5 \log \cos Z_R$, where ρ_B is the air density at the beginning height, v_∞ the initial velocity, and Z_R the zenith distance of the radiant), but its meaning could still be misunderstood (Verniani, 1967a, b). Thus, throughout this paper, I will use plots of the number of meteors at the beginning height (h_B) against the initial velocity (v_∞). The points of the same number of meteors are connected in these plots by the "equinumber" lines. This, of course, is more direct, but we shall see that the results are practically the same as those obtained with the k_B parameter. I have included new data on the different meteor groups.

This paper is based on many hundreds of plots similar to Figures 1 through 11. The observational results from these distribution diagrams are drafted with the use of a light table, and the meteor distributions plotted for different parameters on different sheets are compared. Although only a few of the plots were chosen for publication, all plots are of equal importance, and the observational evidence presented in this paper is based on a complete review of the information from all plots.

This work was supported in part by contract NSR 09-015-033 from the National Aeronautics and Space Administration, and was accomplished while the author held a National Research Council Postdoctoral Visiting Research Associateship supported by the Smithsonian Institution.

The paper is divided into two parts: the observational facts and the interpretations. I feel that the observational facts are more important and that other interpretations may be available in the near future.

2. OBSERVATIONAL FACTS

2.1 The h_B-v_∞ Plot for McCrosky-Posen Super-Schmidt Meteors

This paper is based on plots similar to Figure 1. The x axis represents the initial velocity v_∞ in kilometers per second, and the y axis the beginning height h_B in kilometers. Figure 1 is also a table of the number of meteors contained in different h_B, v_∞ intervals. The h_B interval is designated to be 2 km, and the v_∞ kilometer-per-second interval is 0.04 in log v_∞. If we connect all the points at which the same number of meteors (5, 10, 15, 20, 30, 40) occur in this table, we get Figure 1. A more precise definition is: the center of the zero-order digit is assumed to be the point at which the number of meteors is obtained.

I choose the McCrosky-Posen Super-Schmidt sporadic meteors (1961) with $\cos Z_R \geq 0.5$. The limits for $\cos Z_R$ are used to avoid the influence of low-inclination trajectories (though this influence is not large, as I have confirmed from a few plots similar to Figure 1 but with different intervals of $\cos Z_R$). The classical showers are not too frequent in the McCrosky-Posen (1961) material. Thus, the original number of all sporadic and shower meteors (2529) is reduced to 1848 sporadic meteors with $\cos Z_R \geq 0.5$. The McCrosky-Posen material is homogeneous because of the narrow limits of the magnitude interval. In addition, the influence of the magnitude on the beginning height (Figure 1) is small.

The data in Figure 1 point clearly to the existence of two different levels of beginning height separated by about 9 to 10 km. This same conclusion was drawn in my previous paper (1967) where the k_B parameter was used; the k_B

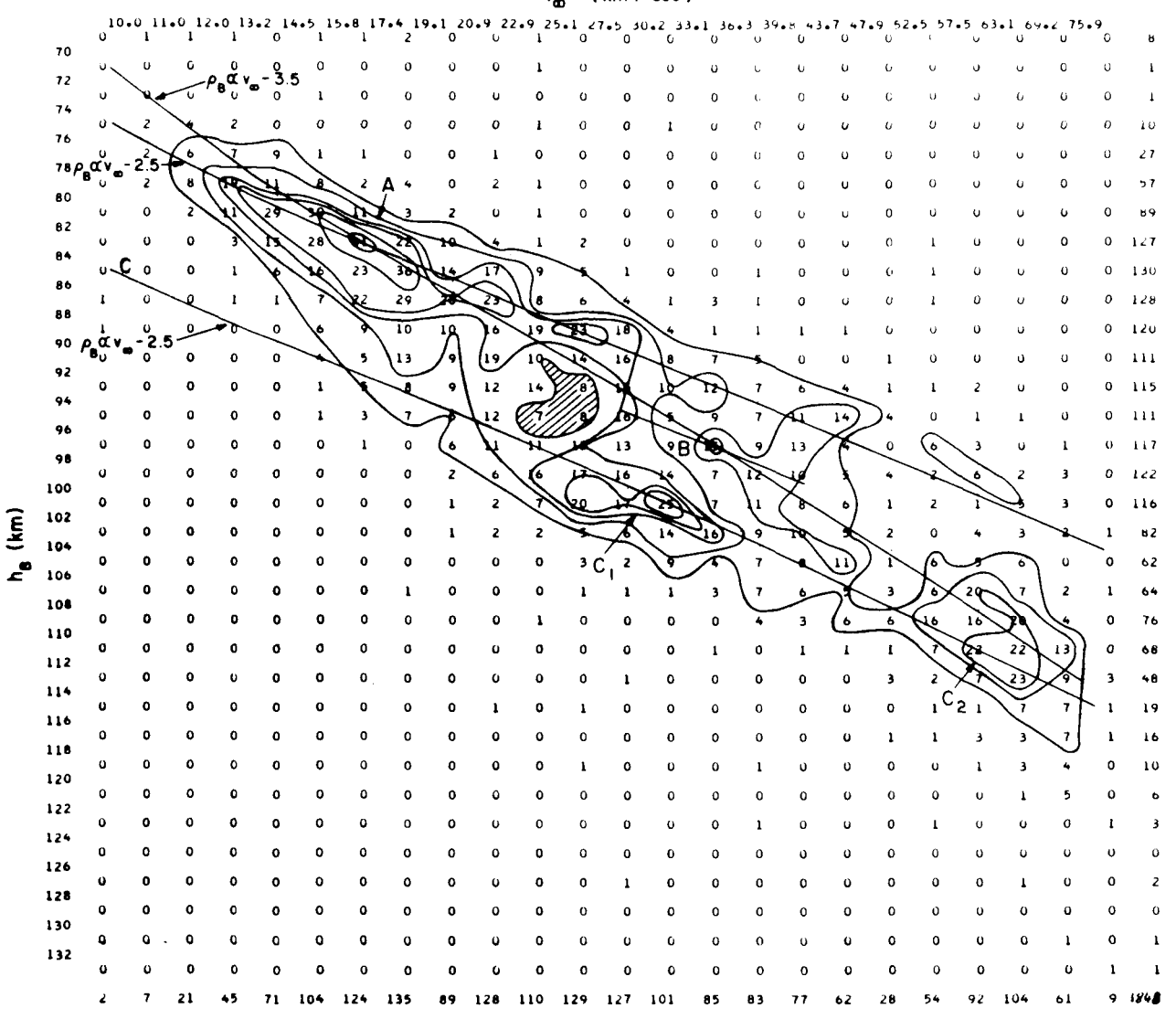

The lines of one exponent are not exactly straight because of the change of the air-density gradient (U. S. Standard Atmospheres, 1962).

Figure 1. McCrosky-Posen sporadic meteors with $\cos Z_R \geq 0.5$ inside two-dimensional intervals of beginning height h_B and initial velocity v_∞. (The center of the zero-order digit is assumed to be the point at which the number of meteors is obtained.)

parameter represents the -2.5 slope ($\rho_B \propto v_\infty^{-2.5}$) in Figure 1. The histograms of k_B (Ceplecha, 1967) are really sums of the numbers of meteors in Figure 1 in the direction of the -2.5 slope. I verified in my earlier paper the -2.5 exponent, using the k_B histograms for different velocity groups. Figure 1 now represents an even better (two dimensional) verification of this exponent. The -3.5 exponent (shown for comparison in Figure 1) found by Jacchia, Verniani, and Briggs (1967) in their extensive statistical studies of Super-Schmidt meteors is more representative of the whole distribution in Figure 1, if this is assumed to be one statistical distribution. I assume that the question of the velocity exponent ($\rho \propto v_\infty^n$) is solved by Figure 1, from which a value close to -2.5 results. After an inspection of Figure 1, it is difficult to accept the value -3.5, so strongly defended by Verniani (1967b), as representative for individual groups.

The notation for the levels in Figure 1 is the same as in my previous paper (1967), namely, A, B, C_1, and C_2 groups. Using this definition, I checked that the A, B, C_1, and C_2 groups are at the positions shown in Figure 1. I wish here to point out clearly that the two main groups found by Jacchia (1958, 1960) were recognized according to the combination of beginning heights with the aphelion distances, which did not enable one to distinguish the A from the C_1 group. The average aphelion distance, Q = 7 a.u., is represented in Figure 1 by a vertical line with $v_\infty \simeq 46$ km sec^{-1} (for Q = 6 a.u., $v_\infty \simeq 44$ km sec^{-1}). Thus, the difference found by Jacchia is equivalent to the difference between the A + C_1 and C_2 groups. It is clear from Figures 1 and 16 that the beginning-height difference is then much lower (3 km as given by Jacchia, 1960) and does not fit the situation in Figure 1. The main reason that Jacchia did not distinguish the A from the C_1 group is evident from Figure 16: the selectional effect of choosing the best (and thus longer and brighter) trajectories from the complete Super-Schmidt material (well represented by McCrosky and Posen, 1961). This resulted in suppression of the A group relative to the C_1 group.

If shower meteors are added to the number of sporadics in Figure 1, the A group is practically unchanged; only the C_1 and C_2 groups are increased. There is, generally speaking, not too much difference, suggesting that the

shower meteors are on the whole similar to the sporadic meteors belonging to the C_1 and C_2 groups.

2.2 Meteor Magnitude Changes in the h_B-v_∞ Plot

The total of 1848 sporadic meteors contained in Figure 1 seems to be high for detailed studies, but the numbers of meteors at single intervals are not much different from 10. Separating all the material into five groups according to the brightness of the meteors, we would mainly have only a few meteors in a single (two-dimensional) interval, which is insufficient for any statistical work. Thus, the studies of h_B-v_∞ diagrams with one additional changing parameter (which is geometrically equivalent to three-dimensional studies) need greater intervals of h_B and v_∞.

I chose h_B intervals of 3 km and log v_∞ intervals of 0.06 (kilometers per second). Figure 2 is then equivalent to Figure 1 and it will be used as a reference to the following figures. Owing to less "resolving power" in Figure 2, the B group is hardly recognized, but it does exist, as we shall see in studying the perihelion distances. Figures 3 to 7 represent the set of plots with decreasing meteor brightness. The C_2 group, which is most important for meteors brighter than 0 mag, becomes almost negligible for meteors fainter than 1.7 mag. The A group is strong enough through the entire studied magnitude interval, but distinctly grows in number for fainter meteors. The C_1 group seems to increase in number from brighter to fainter objects down to 1.7 mag; for fainter objects, the decrease of C_1-group meteors is evident.

The C_2-group meteors have greater velocities than the combined A + C_1 group. Hence, the average masses derived from the luminous equation decrease greatly and systematically from the combined A + C_1 group to the C_2 group, since our observational material is limited by narrow magnitude intervals. Thus, if A, C_1, and C_2 groups are not used separately, each linear least-squares fit among log ρ_B, log v_∞, and log m_∞ (see Figures 3 to 7) results in misleading exponents (as was the case in Jacchia et al., 1967).

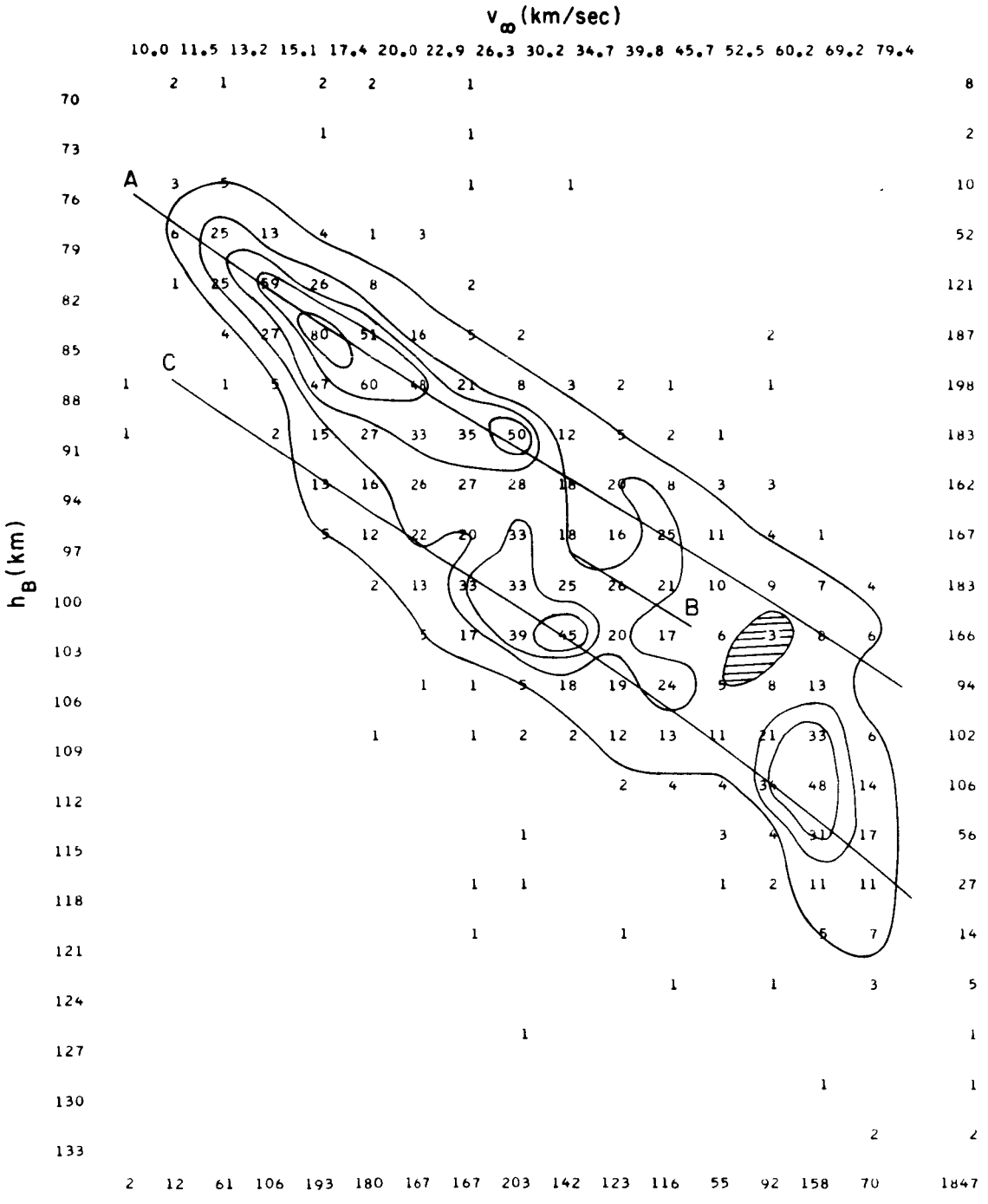

Figure 2. The same h_B-v_∞ plot as in Figure 1, but with 50% bigger intervals. This figure could be directly compared with some further similar plots with additional conditions for the selection of meteors. The A and C levels with -2.5 velocity exponent are plotted.

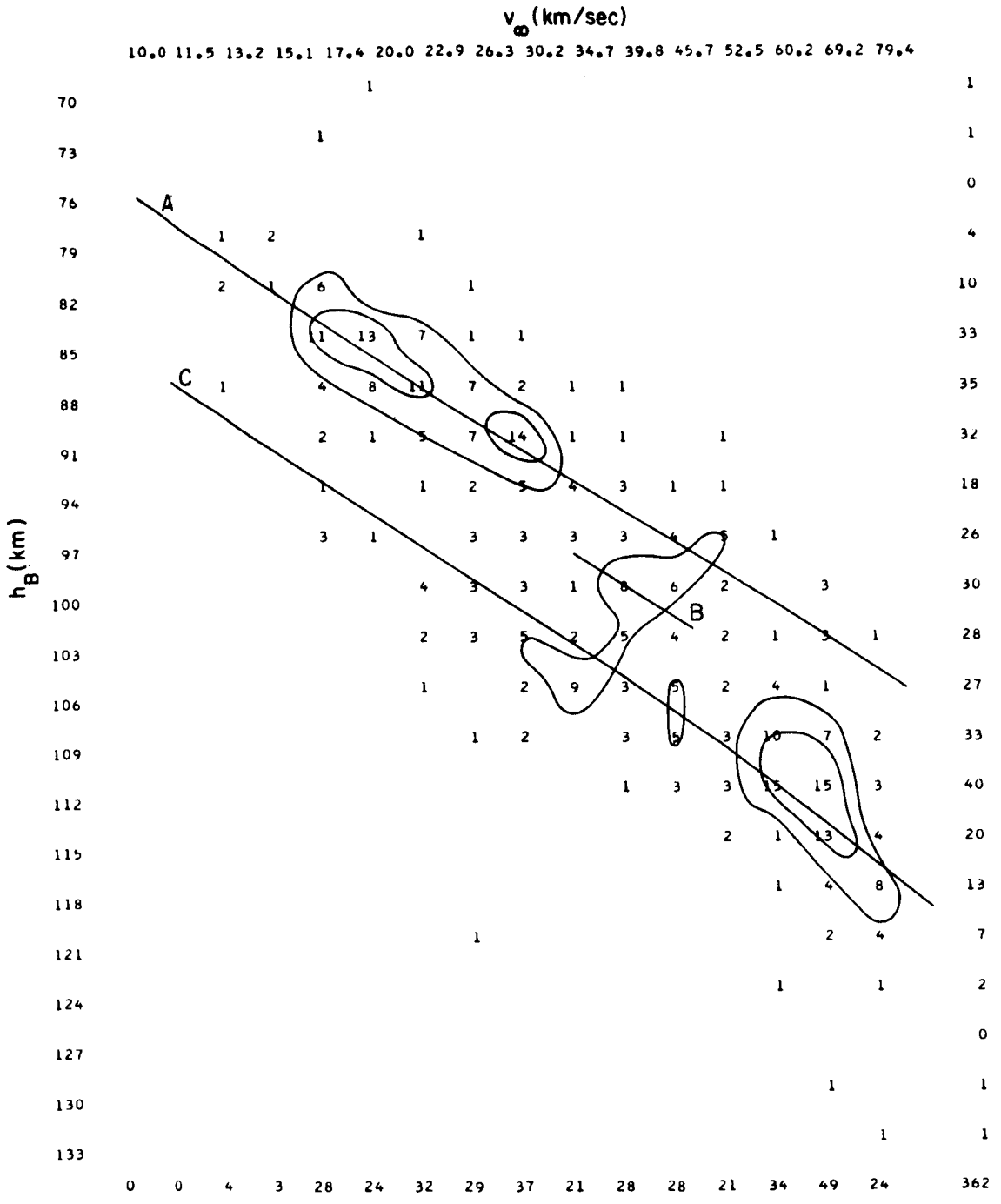

Figure 3. The McCrosky-Posen sporadic meteors with $\cos Z_R \geq 0.5$ and maximum magnitude M brighter than 0. The same plot as Figure 2, with A and C levels the same.

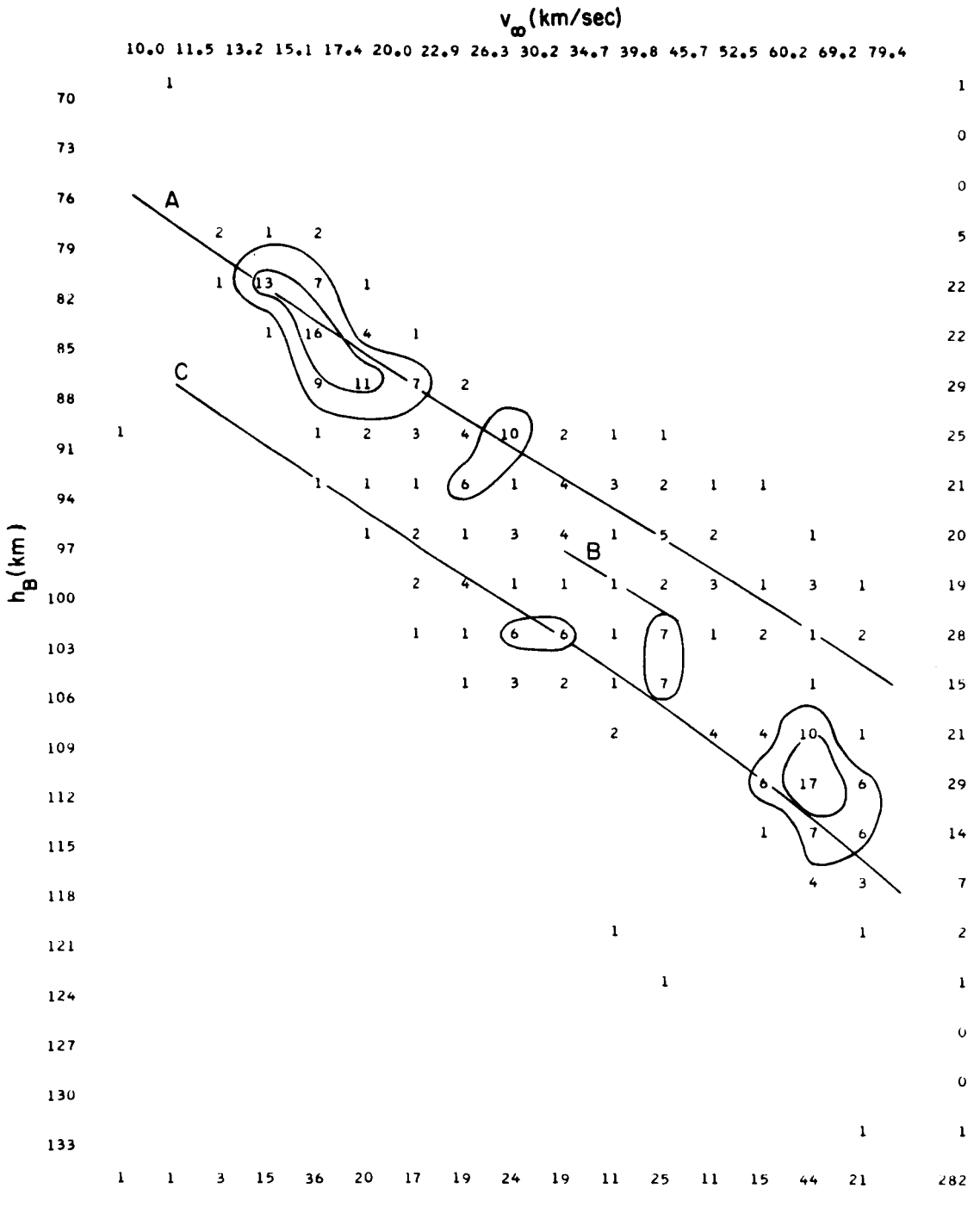

Figure 4. The same as Figure 3, but with meteor magnitudes from 0 to 0.5. The A and C levels are the same as in Figure 2.

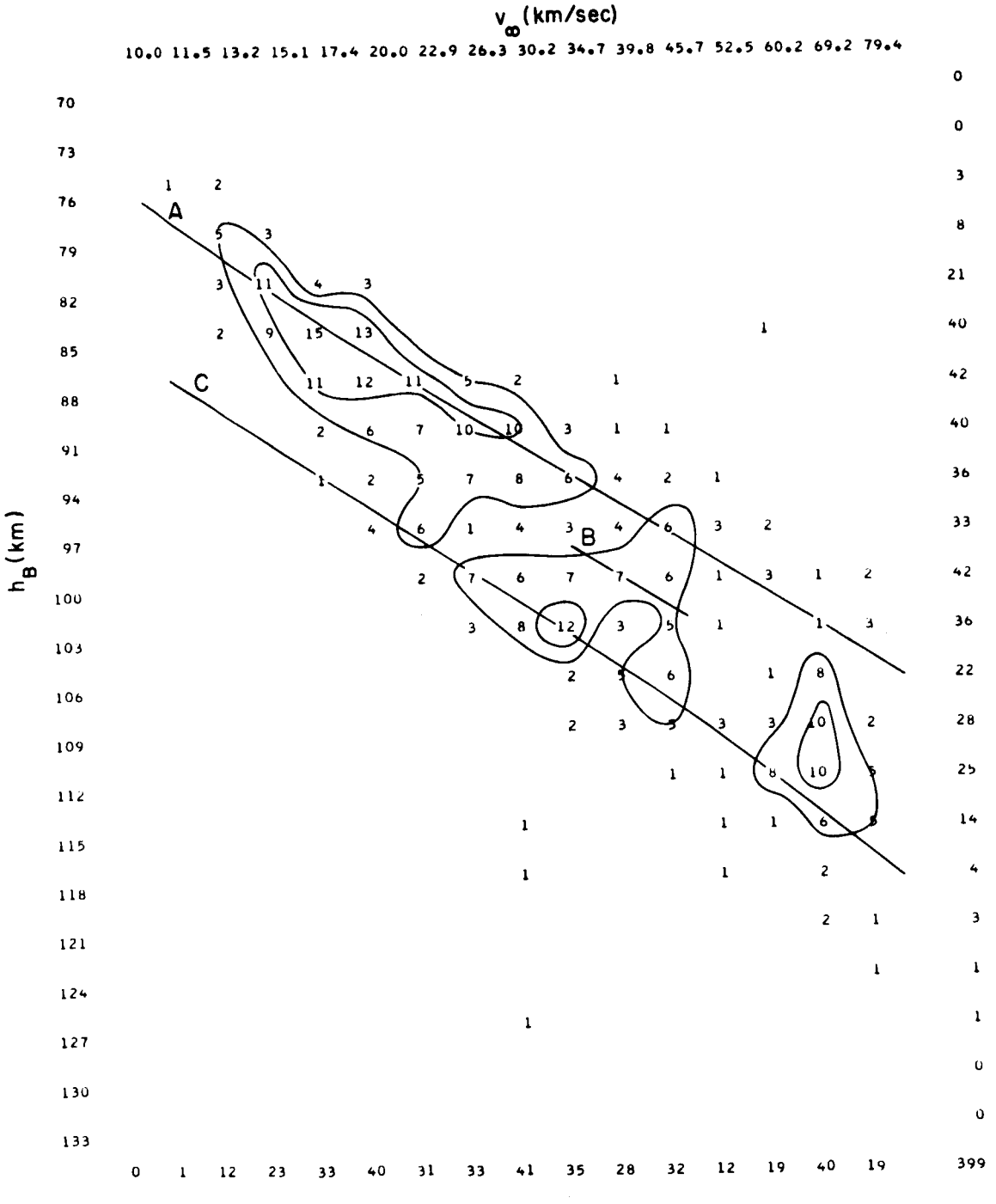

Figure 5. The same as Figure 3, but with meteor magnitudes from 0.5 to 1. The A and C levels are the same as in Figure 2.

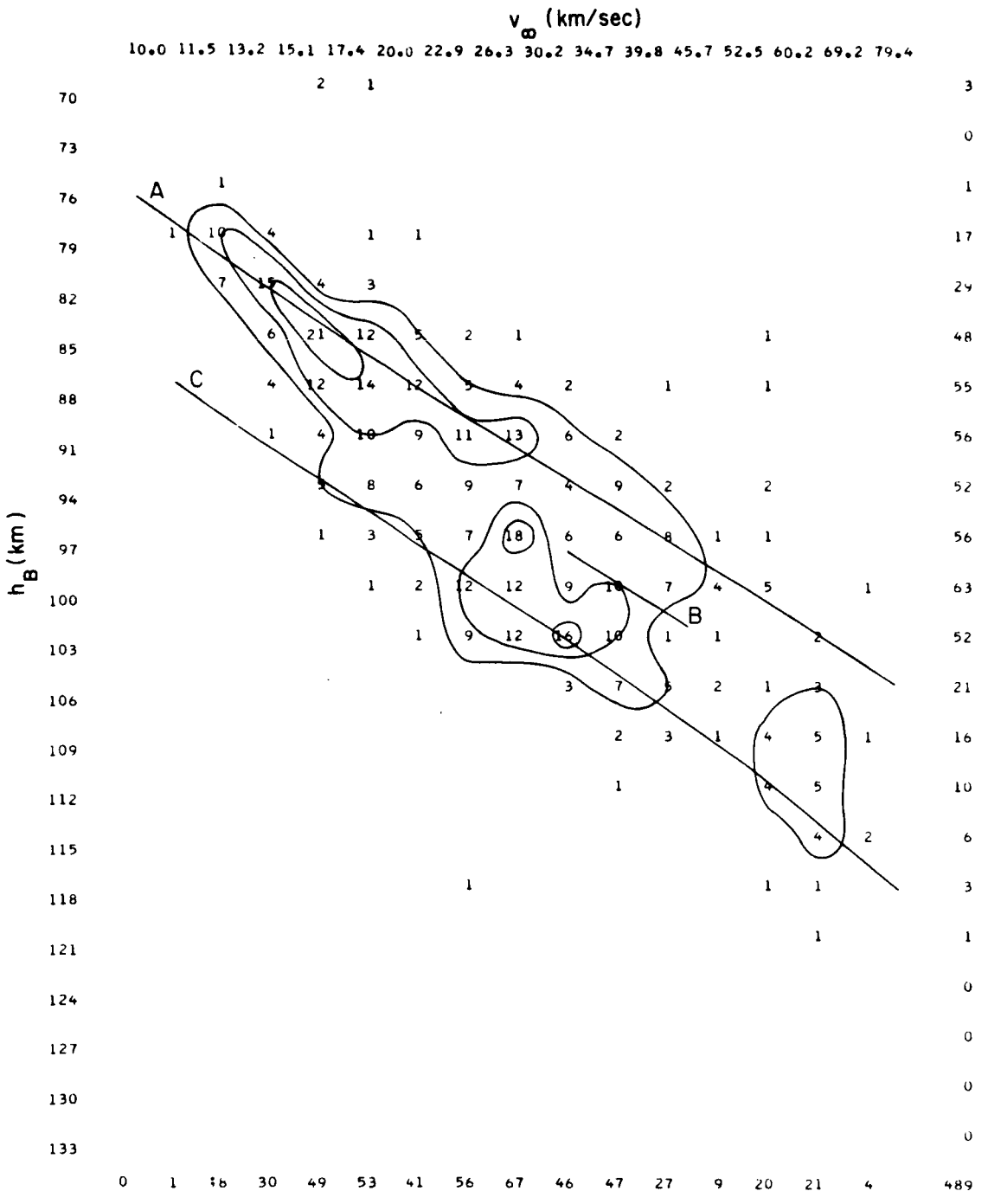

Figure 6. The same as Figure 3, but with meteor magnitudes from 1 to 1.7. The A and C levels are the same as in Figure 2.

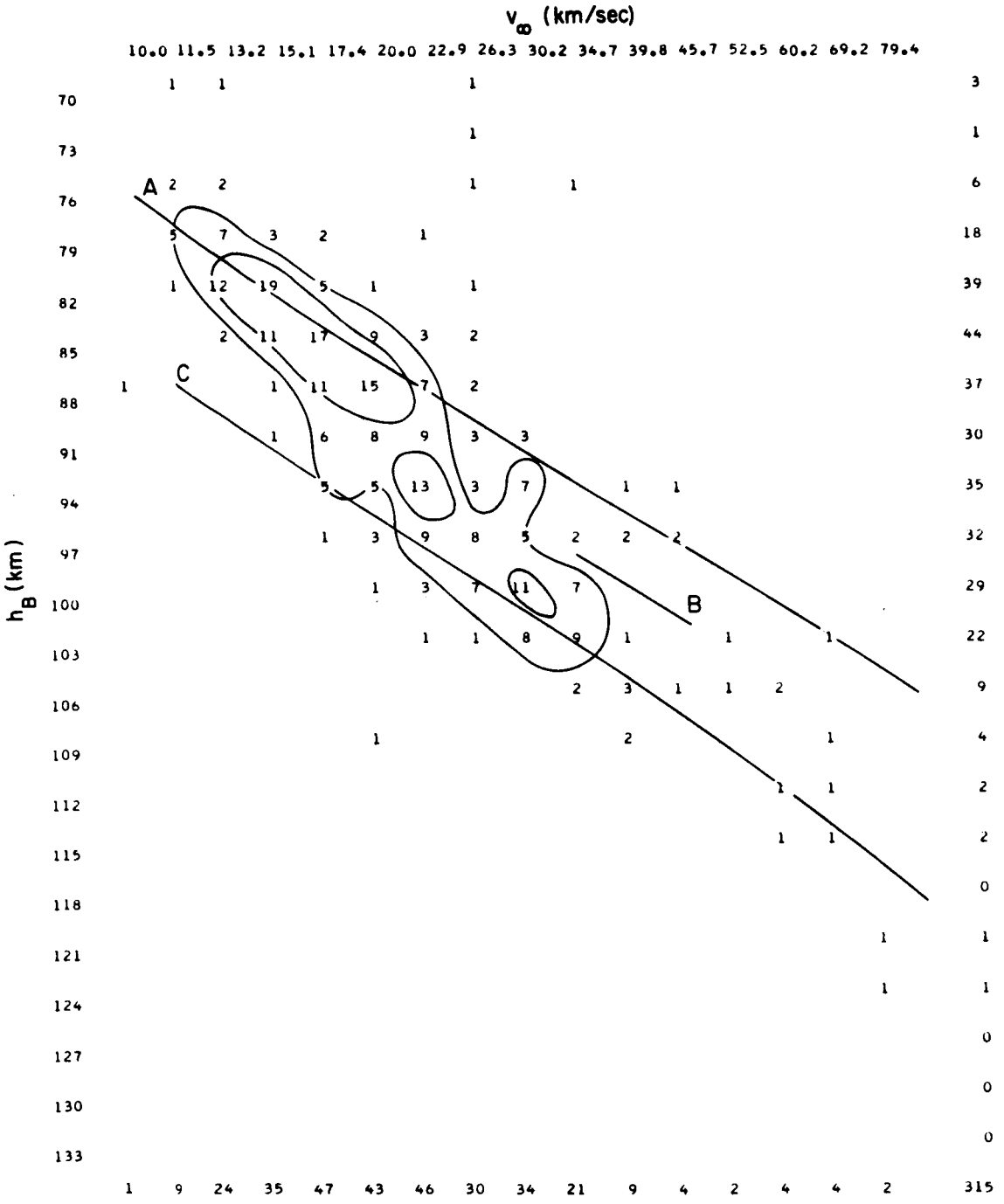

Figure 7. The same as Figure 3, but with meteor magnitudes fainter than 1.7. The A and C levels are the same as in Figure 2.

2.3 Cosmic Weights in h_B-v_∞ Plots

If Figure 2 is constructed from the sum of cosmic weights inside the h_B, v_∞ interval (McCrosky and Posen, 1961), instead of from meteor numbers, we get Figure 8. Figures 2 and 8 differ little in respect to the two levels of beginning height separated by 9 km. It is especially important that in Figures 2 and 8 both levels are simultaneously distinctly present in velocity intervals from 20 to 40 km sec^{-1}.

The C_2 group seems to be so strong in Figure 2 only because of the high probability that these meteors will appear (if the definition of cosmic weight has the correct exponent at v_∞). Figures 2 and 8 suggest that both the levels are present in the whole dynamic range of meteor velocities and that only their relative importance is changed with the initial velocity of the meteor.

2.4 Orbital Elements in h_B-v_∞ Plots

I plotted the h_B-v_∞ diagram by choosing various intervals of different orbital elements. By this procedure I confirmed the results on orbital-element distribution of individual groups as they were derived in my recent paper (Ceplecha, 1967; see especially pp. 38-45). I present here only a clear indication of the existence of the small B group at the intermediate level of beginning height. Figure 9 contains all the sporadic meteors with perihelion distances less than 0.25, and can be compared with Figure 10 containing all sporadic meteors with perihelion distances from 0.25 to 0.5. The great majority of meteors in Figure 9 are of the B group. Few of the B group appear in Figure 10, where the C_1 and A groups are predominant and the C_2 group begins to be distinguished. Similar plots for greater perihelion distances show continuous increase in meteors belonging to the A and C_2 groups. Differences in cosmic weights for the B-group meteors cannot explain Figure 9.

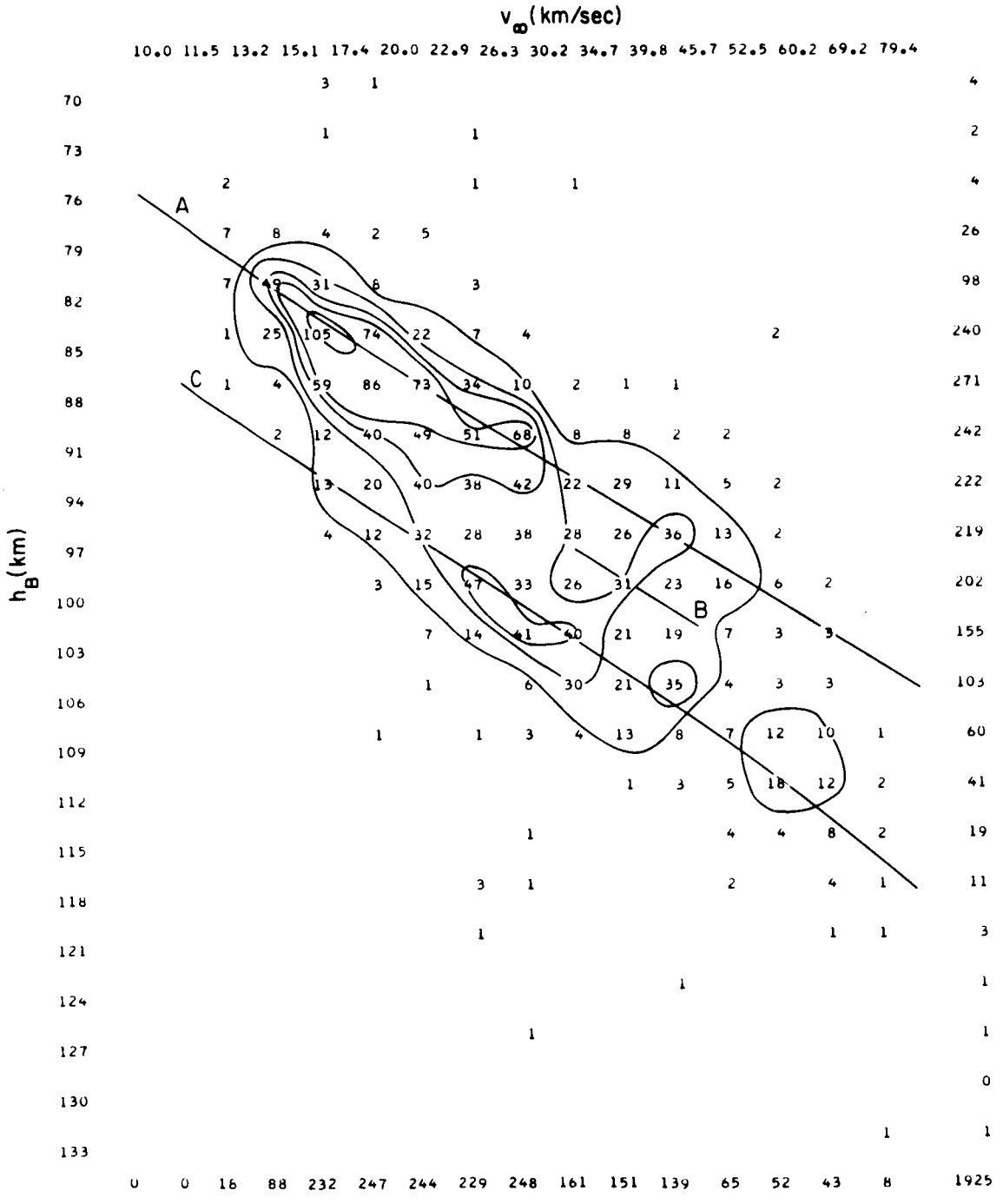

Figure 8. Sums of cosmic weights for McCrosky-Posen sporadic meteors with cos $Z_R \geq 0.5$ inside a two-dimensional interval of h_B, v_∞. Lines of the same cosmic weights are plotted. The A, B, and C levels of the -2.5 velocity exponent are given at the same position as in Figure 2.

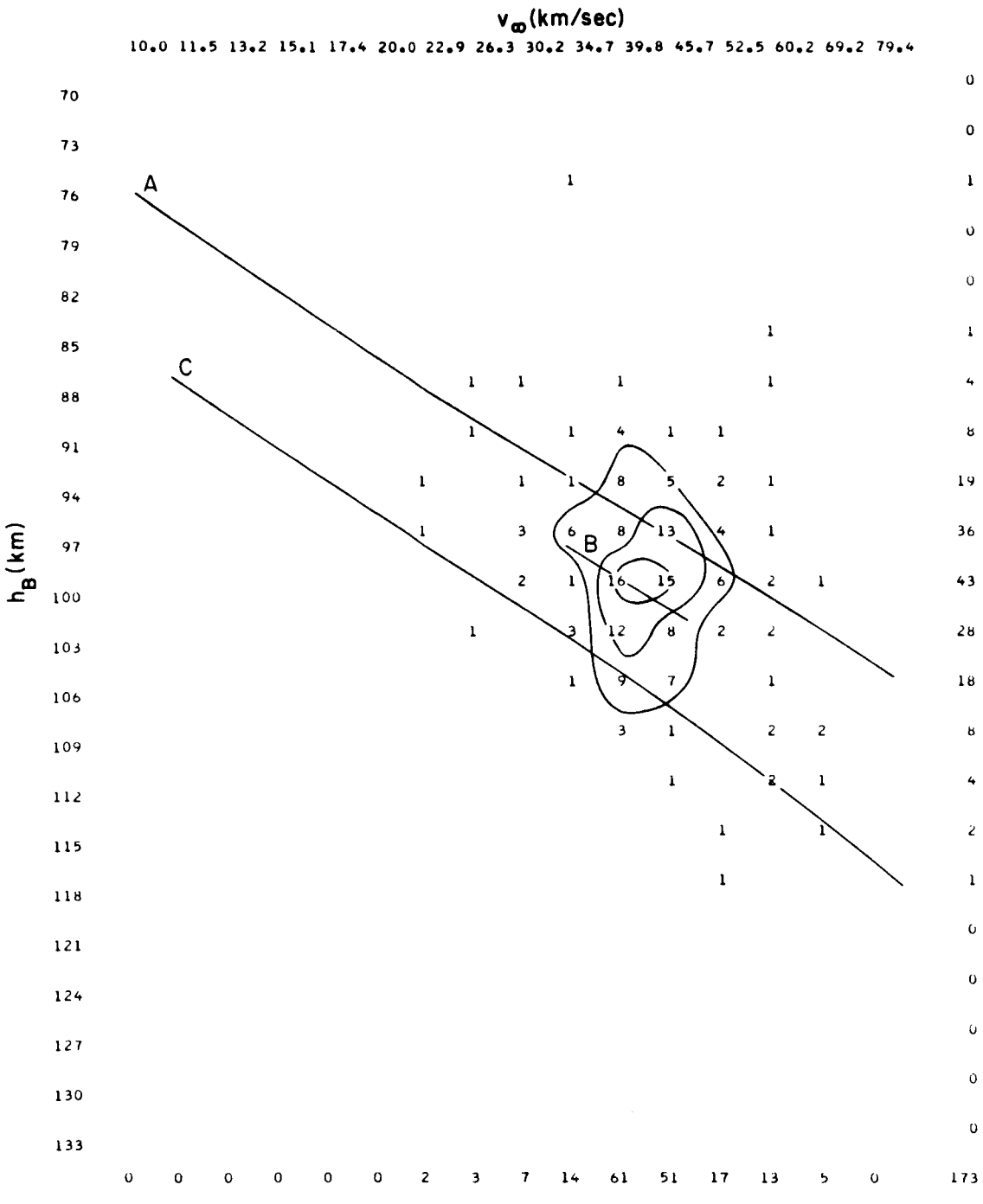

Figure 9. The sporadic meteors with perihelion distances less than 0.25 belong to the B group (McCrosky-Posen sporadic meteors cos $Z_R \geq 0.5$).

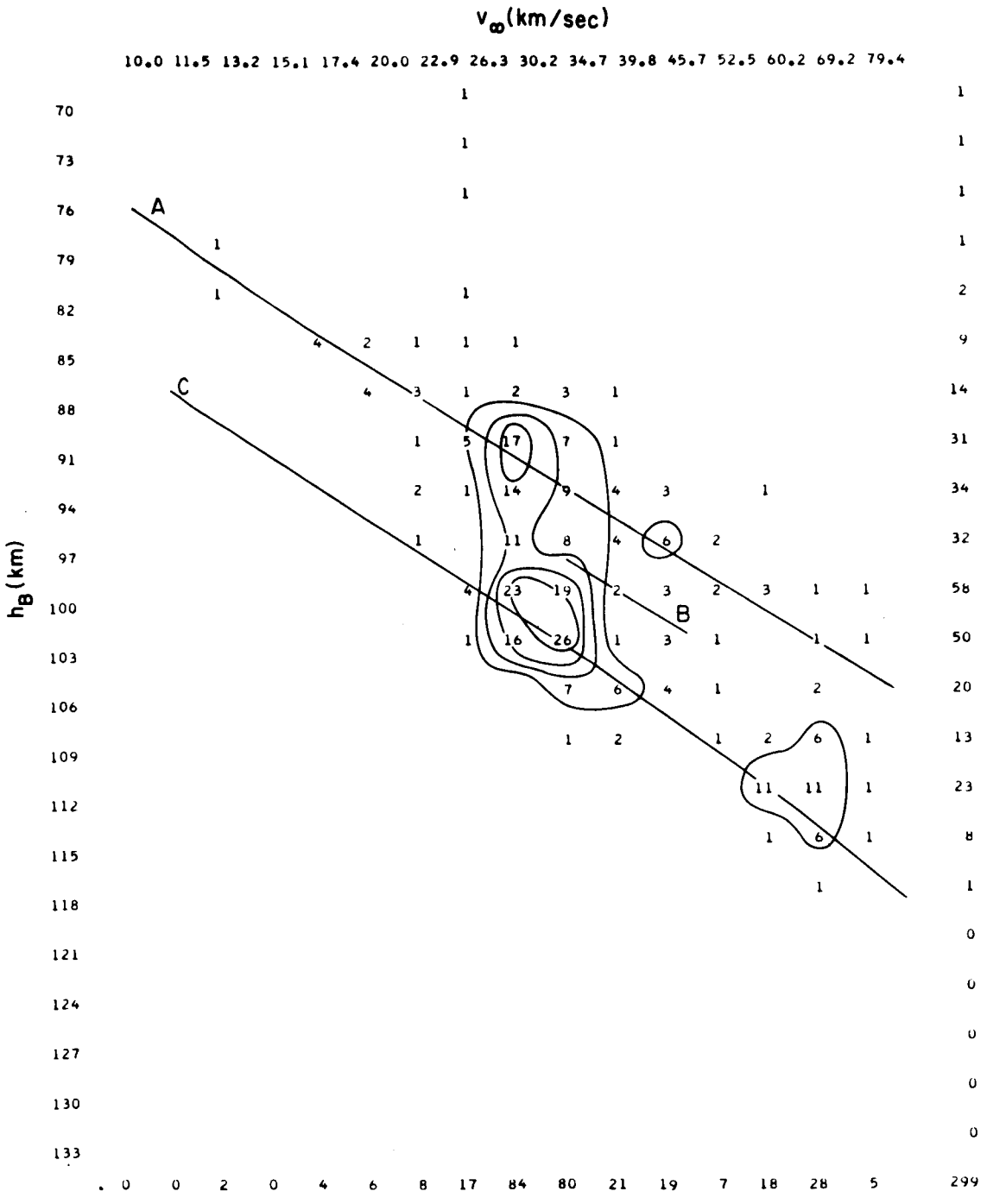

Figure 10. The same plot as Figure 9, but sporadic meteors with perihelion distances from 0.25 to 0.5 belong to the A and C groups only (McCrosky-Posen sporadic meteors with cos $Z_R \geq 0.5$ and with $0.25 \leq q < 0.5$).

The aphelion distance, Q, is used as a parameter for the h_B-v_∞ plot (aphelion distance was not used in my 1967 paper), which gives the following results: for Q < 2 a. u., only the A group is present; for Q = 2 to 3 a. u., the A group is overwhelming and the C_1 group starts to form; for Q = 3 to 4 a. u. and 4 to 5 a. u., the A group is about 60% and the C_1 group 40%; for Q = 5 to 6 a. u. and 6 to 7 a. u., the A group is about 50% and the C_1 group 50%; for Q > 7 a.u., the situation is completely different — the A group is 20%, the C_1 group 35%, and the C_2 group 45%. If we consider that the precision of individual values of Q in the McCrosky-Posen data is not good, especially for Q > 4 a. u., the statistical separation of A, C_1, and C_2 by means of aphelion distance is evident. The separation of combined A + C_1 from C_2 by means of aphelion distance and beginning height was recognized previously by Jacchia (1958).

2. 5 Seasonal and Diurnal Variations

Since seasonal and diurnal variations might be a possible explanation for the existence of the two main levels of beginning height, I used the h_B-v_∞ diagrams constructed for different seasons (January to March, April to June, July to September, October to December) and different times of the day (< 0. 2 of UT day, 0. 2 to 0. 25, 0. 25 to 0. 30, 0. 30 to 0. 35, 0. 35 to 0. 40, > 0. 40). The most important conclusion from all the plots is that both main levels of beginning height exist at all seasons and during the whole night simultaneously.

There are, of course, changes in the relative numbers of meteors belonging to different groups. In spring and summer, A-group meteors dominate; in autumn, the C_2 group dominates; and in winter, there is approximately the same number of meteors in the A, C_1, and C_2 groups. The evening hours have only the A and C_1 groups because of the strong geocentric velocity selection; the C_2 group starts to form after midnight, and in the morning of a winter day it is the strongest group because of the geocentric velocity selection.

Of all the figures, the most instructive is Figure 11, which contains meteors of early morning hours (> 0.40 of UT day), chiefly in the winter season. The three groups are clearly presented in Figure 11, which indicates that the seasonal and diurnal variations of beginning height cannot explain the existence of the two main levels of beginning height.

The h_B-v_∞ plots were also made for different magnetic indexes measured at Tucson. The actual magnetic indexes at the passage of each meteor were used. Whether the intervals are magnetically quiet or disturbed, the two beginning-height levels A and C coexist.

2.6 Average Orbital Elements Along the A and C Lines

We can also examine the orbital elements of meteors of individual groups in a different manner. The h_B-v_∞ diagram can be used and the particular average element at each interval can be plotted instead of the numbers of meteors. Then we can plot lines of the same average values of the orbital element considered. We can also follow the A and C lines of Figure 1 ($\rho_B \propto v_\infty^{-2.5}$) and look for the changes in each element. The most interesting results are presented in Figures 12 to 15.

The numbers of meteors (inside an interval of 2 km in h_B and 0.04 in log v_∞) along the A, B, and C lines of Figure 1 are plotted in Figure 12. The x axis is log v_∞, but h_B changes as we follow the A and C lines of Figure 1. Figure 12 shows the influence of statistical spread, which is due to the inaccuracy of the material and causes the interference of the A, B, and C levels. But the differences in meteor numbers of the groups are distinct. The average smooth reciprocal semimajor axis of the meteor orbits (1/a) is plotted in Figure 13. Again, the average was followed along the A, B, and C lines of Figure 1. A similar plot for the inclination is given in Figure 14. There is little difference in the inclinations between A and C up to v_∞ = 40 km sec^{-1}. The high-inclination orbits with v_∞ > 40 km belong to the C_2 group. The differences between A and C groups in the semimajor axis (Figure 13) are greater. The orbits are shorter along the A than along the C line.

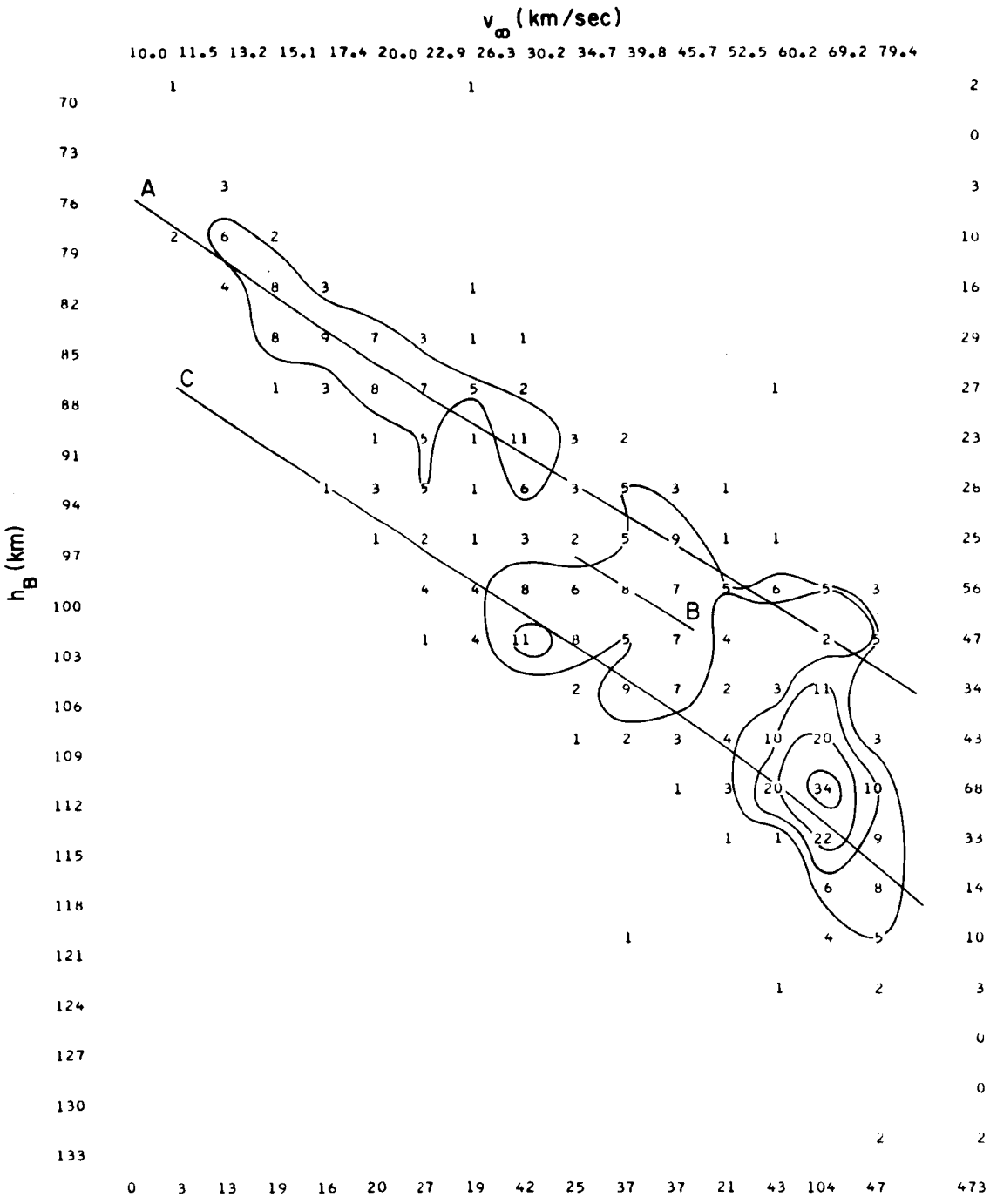

Figure 11. The McCrosky-Posen sporadic meteors photographed in early morning hours (T > 0.40 of UT day) show both the A and C levels, which excludes the daily- and seasonal-variation explanation of the levels.

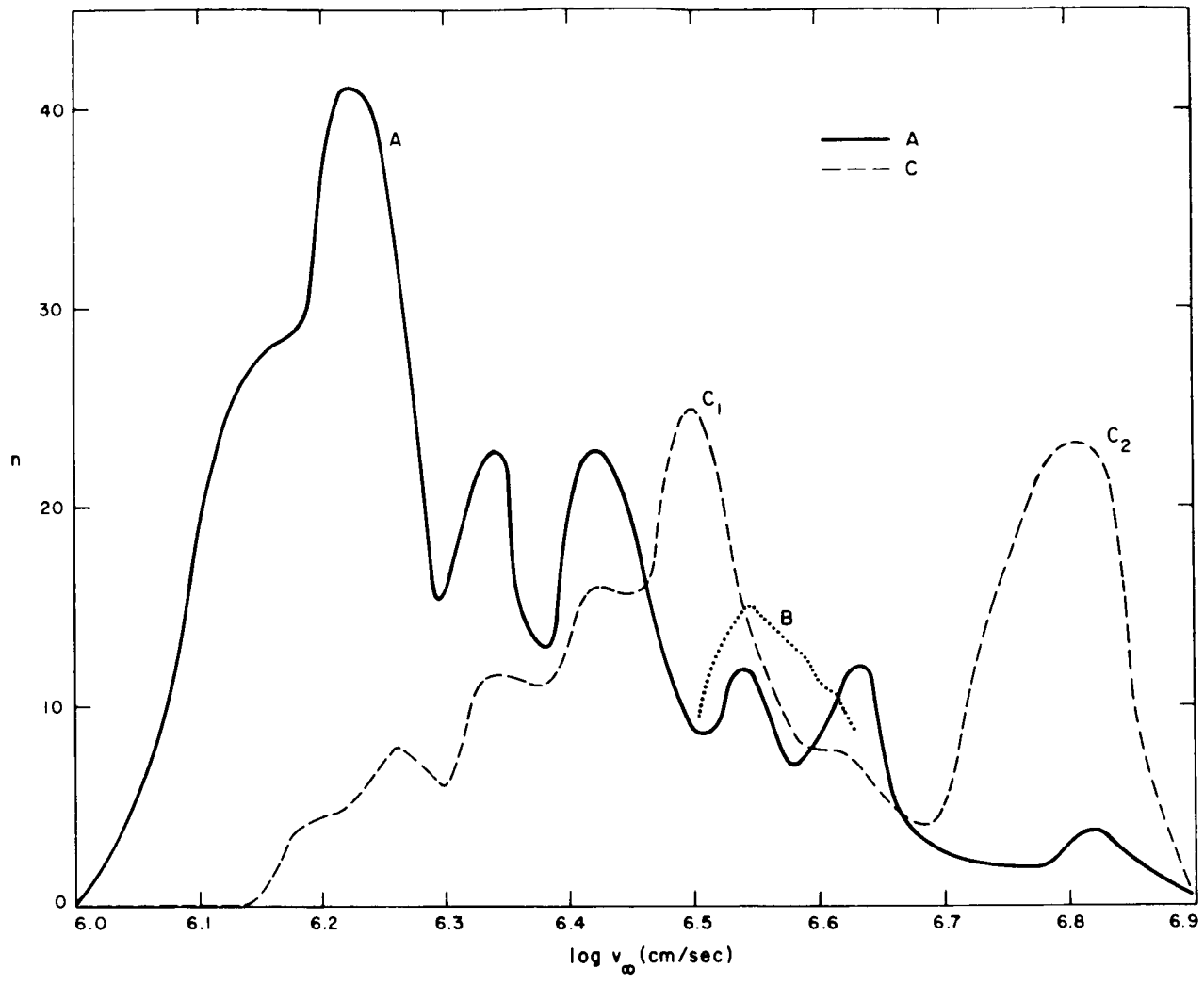

Figure 12. Number of meteors n along the A, B, and C lines of Figure 1 is plotted against log v_∞. (McCrosky-Posen sporadic meteors with cos $Z_R \geq 0.5$.)

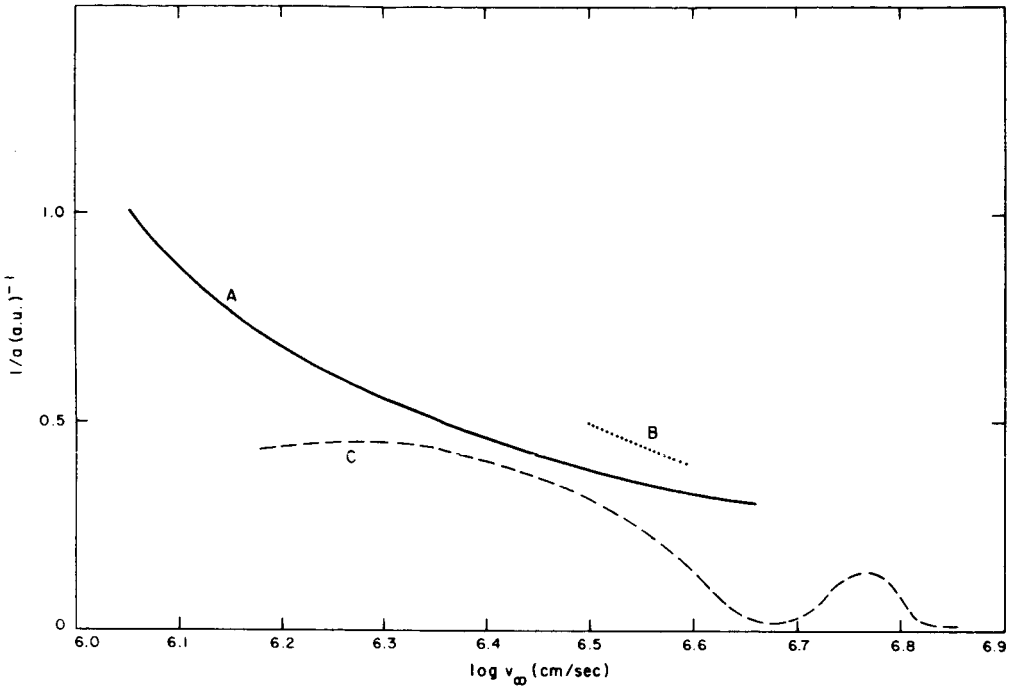

Figure 13. The average reciprocal semimajor axis along the A, B, and C levels of Figure 1 is plotted against the log v_∞. (McCrosky-Posen sporadic meteors with cos $Z_R \geq 0.5$.)

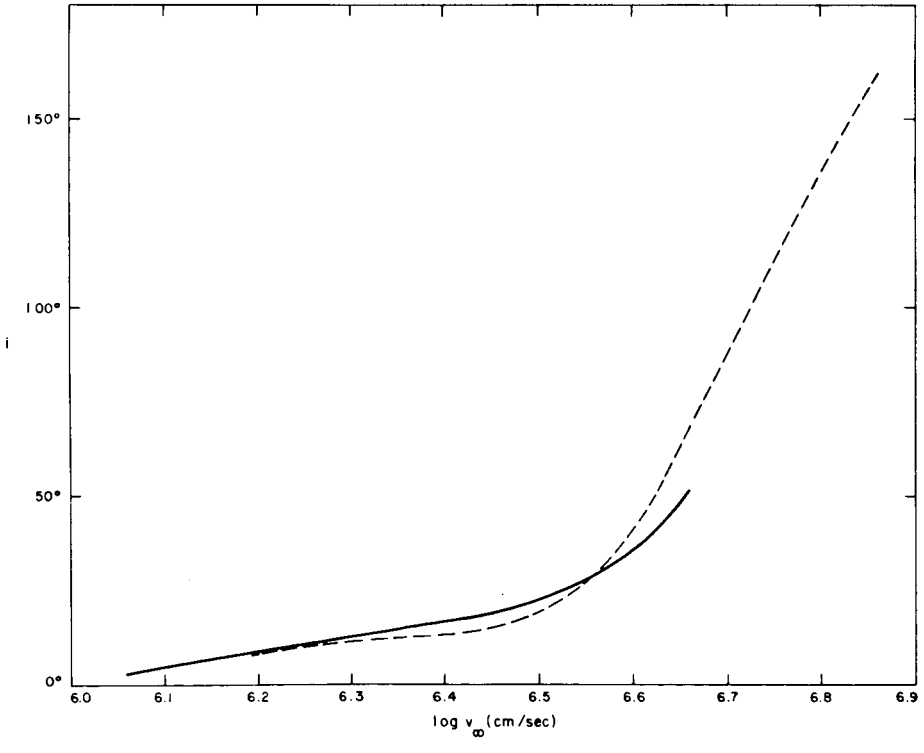

Figure 14. The average orbital inclination along the A, B, and C levels of Figure 1 is plotted against the log v_∞.

The most surprising is the plot of average perihelion distances q in the h_B-v_∞ diagram (Figure 15). The area of minimum values of q is clearly connected with the B group. A similar plot for the average cosmic weight shows nothing special in the same B-group area. Either the cosmic-weight formula fails in this area on the h_B-v_∞ diagram, or Figure 15 reflects the real distribution. The minimum of perihelion distance is connected with the local maximum of number of meteors (B group). Thus, for some reason, the small perihelion distance probably causes these meteors to begin between the A and C levels.

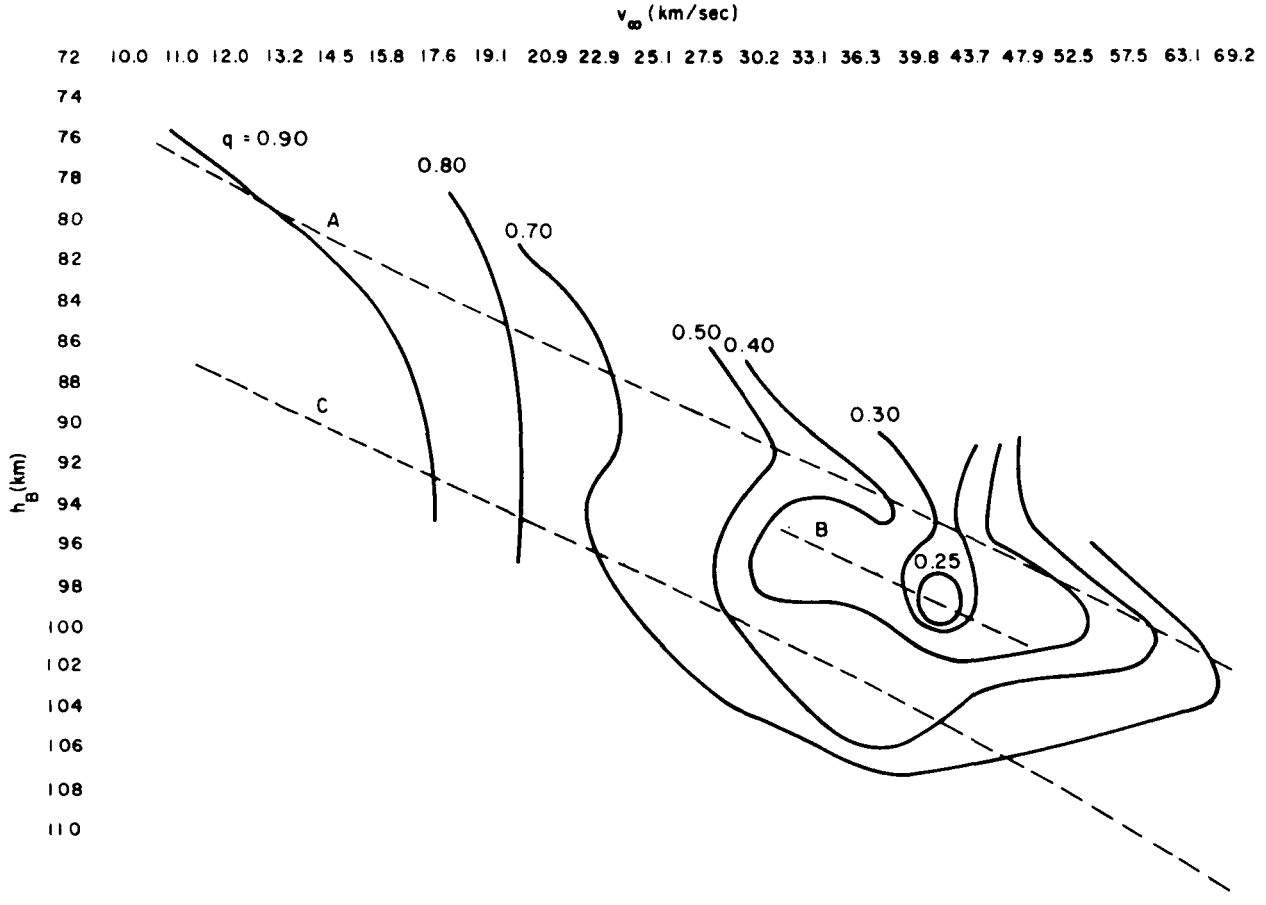

Figure 15. The average perihelion distance is given in the h_B-v_∞ plot. The A, B, and C levels of Figure 1 are shown by dotted lines. One would expect vertical lines connecting the same average perihelion distances if only one statistical group is present, but the plot verifies a strong dependence of this quantity on the beginning height. (McCrosky-Posen sporadic meteors with $\cos Z_R \geq 0.5$.)

The regular distribution of any element in a plot similar to Figure 15 should be a vertical line, as one would expect. This means that one can expect average elements to be different for different initial velocities. But if the beginning heights are spread only statistically because of errors of measurement, there could hardly be any change of average element with beginning height. Figure 15 shows just the opposite in some parts, verifying that differences in beginning height are due to some physical cause. The plots similar to Figure 15 for other elements show the same anomalies, but not so strikingly. The plot of average inclination is the most regular, having only small deviations from the vertical lines; the eccentricity plot shows greater deviations from regularity; the semimajor-axis plot shows even greater deviations; the aphelion-distance plot is similar to the semimajor-axis plot; and the perihelion-distance plot (Figure 15) is completely different from the regular expected distribution.

2.7 Jacchia's Super-Schmidt Meteors in the h_B-v_∞ Plot

The preceding sections dealt with the McCrosky-Posen sporadic meteors. It is useful to look at a precisely reduced selection from the same material published by Jacchia et al. (1967; also referred to as Jacchia's meteors). We will also inspect the problem of differences between the "dynamic" and the "photometric" mass in the h_B-v_∞ diagram.

The data on Jacchia's meteors are more precise than those of McCrosky-Posen, but if we take all the meteors (including showers) and omit those with $\cos Z_R < 0.5$, we have only 317 cases. Thus, only the low-resolution intervals (h_B = 3 km and $\log v_\infty = 0.06$) were used. Figure 16 shows the influence of selection (cf. Figure 2): The A group is a rather large diffuse area, the C_1 group is dominant (partly due to showers), and the C_2 group is well defined. This distribution was caused by the fact that A-group meteors have much shorter trajectories with lengths less than 12 km (see Section 2.12), while the C_1 and C_2 groups have trajectory lengths greater than 12 km. The main purpose of Jacchia's selection was to obtain the best possible decelerations; thus longer trajectories with many rotating shutter dashes were strongly

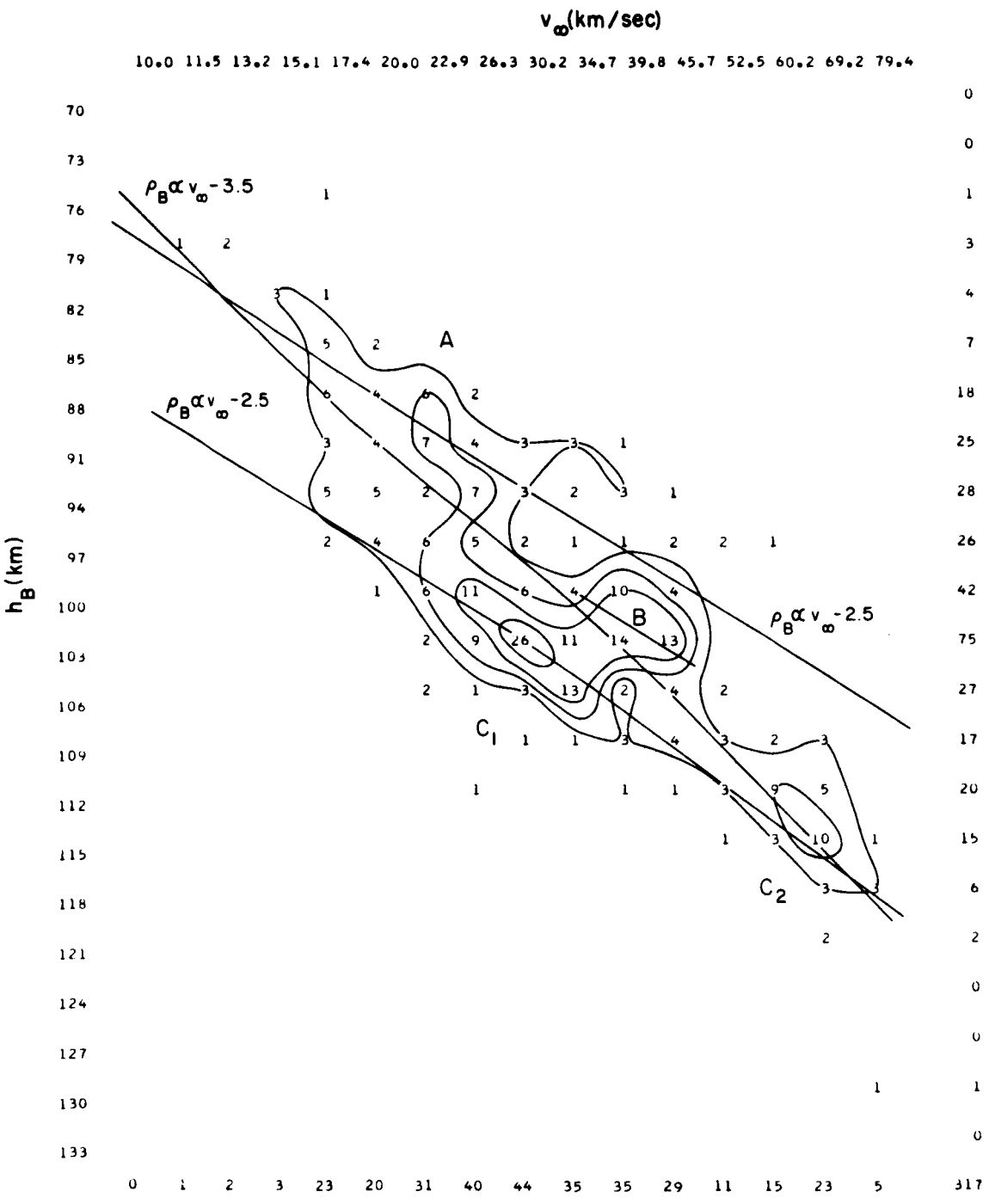

Figure 16. Jacchia's Super-Schmidt meteors in the same plot as Figure 2. The A, B, and C levels of the -2.5 velocity exponent are plotted 2 km higher than in Figure 2. The -3.5 velocity exponent is given for comparison. Jacchia's selection from the complete Super-Schmidt material resulted in marked suppression of the A group. (All Jacchia's meteors with $\cos Z_R \geq 0.5$.)

preferred. On an average, Jacchia's meteors are brighter than the McCrosky-Posen meteors. Thus, even without the above selection, the distribution would be more similar to the distribution of small-camera meteors (see Section 2.10). The effect of brightness also caused Jacchia's meteors to begin about 2 km higher on an average than the McCrosky-Posen meteors (Figure 2 vs. Figure 16). We are thus able to explain why the A group in Jacchia's material is so markedly suppressed. But, using the h_B-v_∞ plot together with the McCrosky-Posen data from Figure 1, we are also able to distinguish statistically the A group in Jacchia's material.

An extensive statistical study of Jacchia's meteors was published (Jacchia et al., 1967), and the results were assumed to represent an average meteor of magnitude interval characteristic for Super-Schmidt cameras. Comparison of Figures 2 and 16 clearly shows that the published results are more representative of the C_1 and C_2 groups than of all the Super-Schmidt meteors.

The velocity exponent -3.5 ($\rho_B \propto v_\infty^{-3.5}$), if related to the air density at the meteor beginning, was derived from meteors in Figure 16. It is obvious from Figure 16 that the line for the -3.5 exponent fits the whole pattern quite well. Since, however, we know from Figures 1 and 2 that there is a statistical distribution represented by two different levels – not by only one, as Jacchia et al. (1967) assumed – the -3.5 exponent is clearly an apparent or unreal value. The levels of the -2.5 exponent are represented in Figure 16. They were plotted from Figure 1, with the beginning height simply increased by 2 km in both cases. It is clear that, without previous knowledge of Figure 1, these two levels would be hard to recognize from Figure 16.

Jacchia used the separation by aphelion distance $Q > 6$ a.u., which is equivalent to the separation of combined A + C_1 from C_2. This is probably also one of the reasons that the difference (3 km) in beginning height between meteors with $Q > 6$ a.u. and $Q \leq 6$ a.u. is found to be much less than the height difference between the A and C levels.

The average masses of Jacchia's meteors derived from light curves are much smaller for the high-velocity C_2 group than for the C_1 group. Jacchia et al. (1967) used for the best fit of beginning heights the mass exponent ($\rho_B \propto v_\infty^n m_\infty^p$). But if the big systematic change in mass in Figure 16 (decreasing from left to right) is considered, the resulting mass exponent is seen to be, rather, a velocity exponent. A very small change of velocity exponent in the luminous equation would have a strong influence on the resulting mass exponent in the relation $\rho_B \propto v_\infty^n m_\infty^p$, simply because of the existence of the grouping at different levels.

We saw in Section 2.2 (Figures 3 to 7) that the C_2 group increases in meteor number with increasing brightness, relative to the other groups. If this corresponds to actual changes in the importance of the groups, then the mass exponent more probably represents these statistics of meteor numbers of individual groups than any real physical change of the h_B with the mass.

2.8 Dynamic and Photometric Masses in the h_B-v_∞ Plot

My recent paper (1966) on the differences between the dynamic (m_d) and the photometric (m_{ph}) mass of a meteor points out clearly the dependence between the k_B parameter and log (m_{ph}/m_d). The meteors used are those of Jacchia et al. (1967) with many precise deceleration measurements necessary for the dynamic mass computation. Therefore, we do not have as much material for the study of the A group (Figure 16) as we would for all Super-Schmidt meteors.

I simply define dynamic mass as

$$m_d = \left(\frac{\rho\, v^2}{-dv/dt} \right)^3 , \qquad (1)$$

putting $(\Gamma A)^3 = 1$ (Γ is the drag coefficient, A is the shape-density factor), where $(\Gamma A)^3$ is a multiplying factor of the right-hand side.* From definition (1), log m_d is a relative value with some unknown constant to be added.

*This definition is the same as the definition of $\Delta \log \rho$ used by Jacchia et al. (1967), except for the multiplying factor.

On the other hand, I define photometric mass as

$$m_{ph} = \frac{2}{\tau_0} \int_t^{\infty} \frac{I dt}{v^3} \quad , \tag{2}$$

which is in complete agreement with the definition of Jacchia et al. (1967); and I use the m_1 values from Table 1.2 of that paper, which are equivalent to the old τ_0 value 6.46×10^{-19} (cgs; I in zero-magnitude units).

I computed log (m_{ph}/m_d) for each point published in their Table 1.2. I used h_B-v_∞ plots with different intervals of log (m_{ph}/m_d) (see Figures 17-20) to point out the close connection between the beginning-height levels and log (m_{ph}/m_d). Almost all values of log (m_{ph}/m_d) are inside a broad interval of -2 to +3. The distribution seems to be far from a uniform statistical distribution (Ceplecha, 1966). If we divide this broad interval into smaller intervals, we get the following results: The log (m_{ph}/m_d) interval from -2 to 0 belongs mainly to the A and B groups (Figure 17); the interval 0 to 0.8 is characteristic for statistical overlap of the A and B groups with the C_1 and C_2 groups (Figure 18); the C_1 and C_2 groups are dominant in the interval 0.8 to 1.5 and only insignificant interference of A and B is present (Figure 19); and the C_1 and C_2 groups are the only ones in the interval 1.5 to 3 (Figure 20).

We must take into account that the log (m_{ph}/m_d) values have at least a 3 times greater statistical spread than do the k_B values (Ceplecha, 1966). Then, if we compare both extreme cases (Figure 17 with Figure 20), we see the complete separation of the A and C groups also on the basis of log (m_{ph}/m_d) values. These results are the same as those obtained by means of the k_B parameter, but the h_B-v_∞ plots are even more instructive for the whole situation.

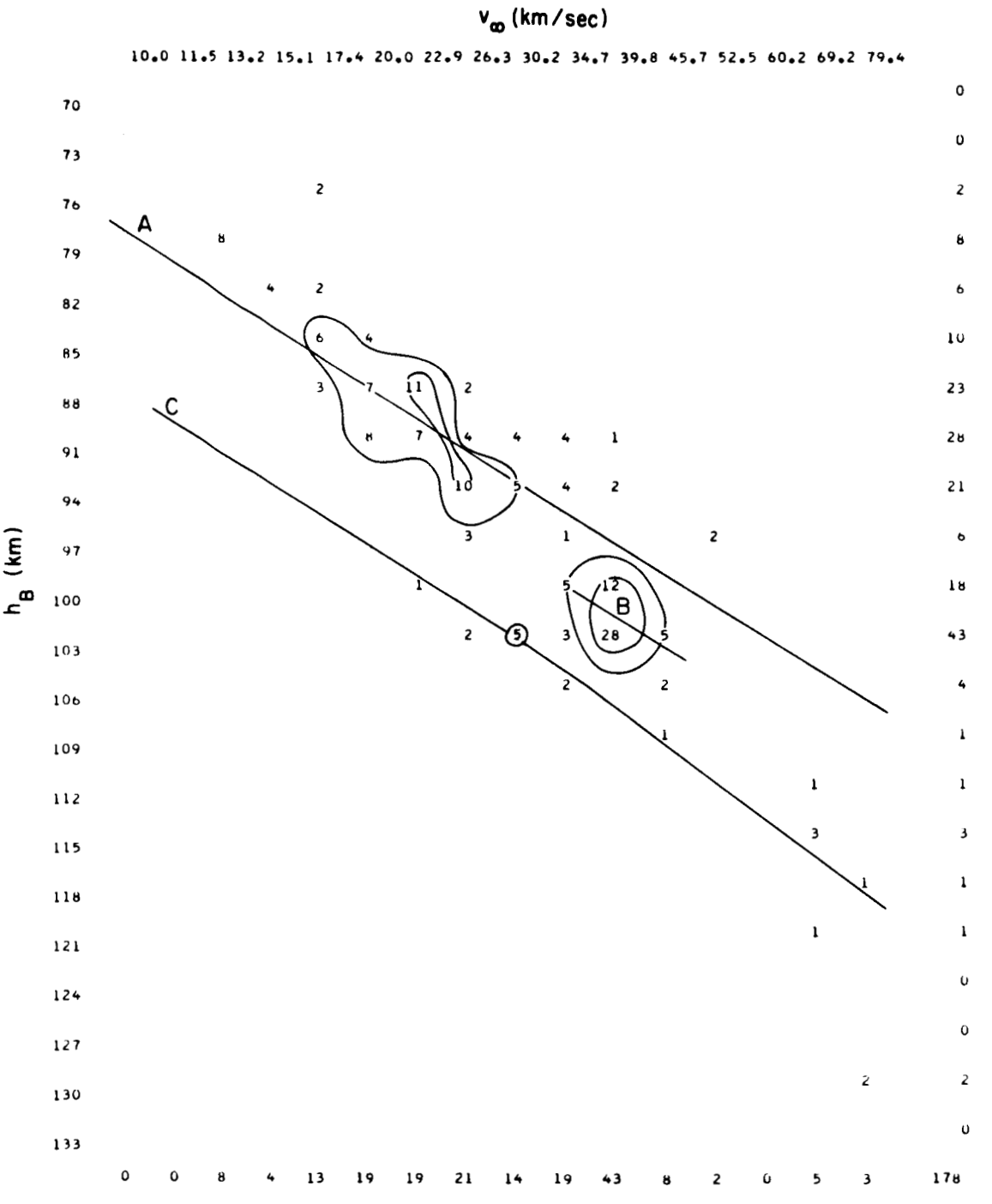

Figure 17. Numbers of Jacchia's meteors, with the difference between photometric and dynamic mass in the interval from -2 to 0 ($-2 \leq \log m_{ph}/m_d < 0$), are given inside two-dimensional intervals of h_B and v_∞. The A, B, and C levels of Figure 16 are shown. The A and B groups are the only ones present. (Jacchia's meteors with $\cos Z_R \geq 0.5$.)

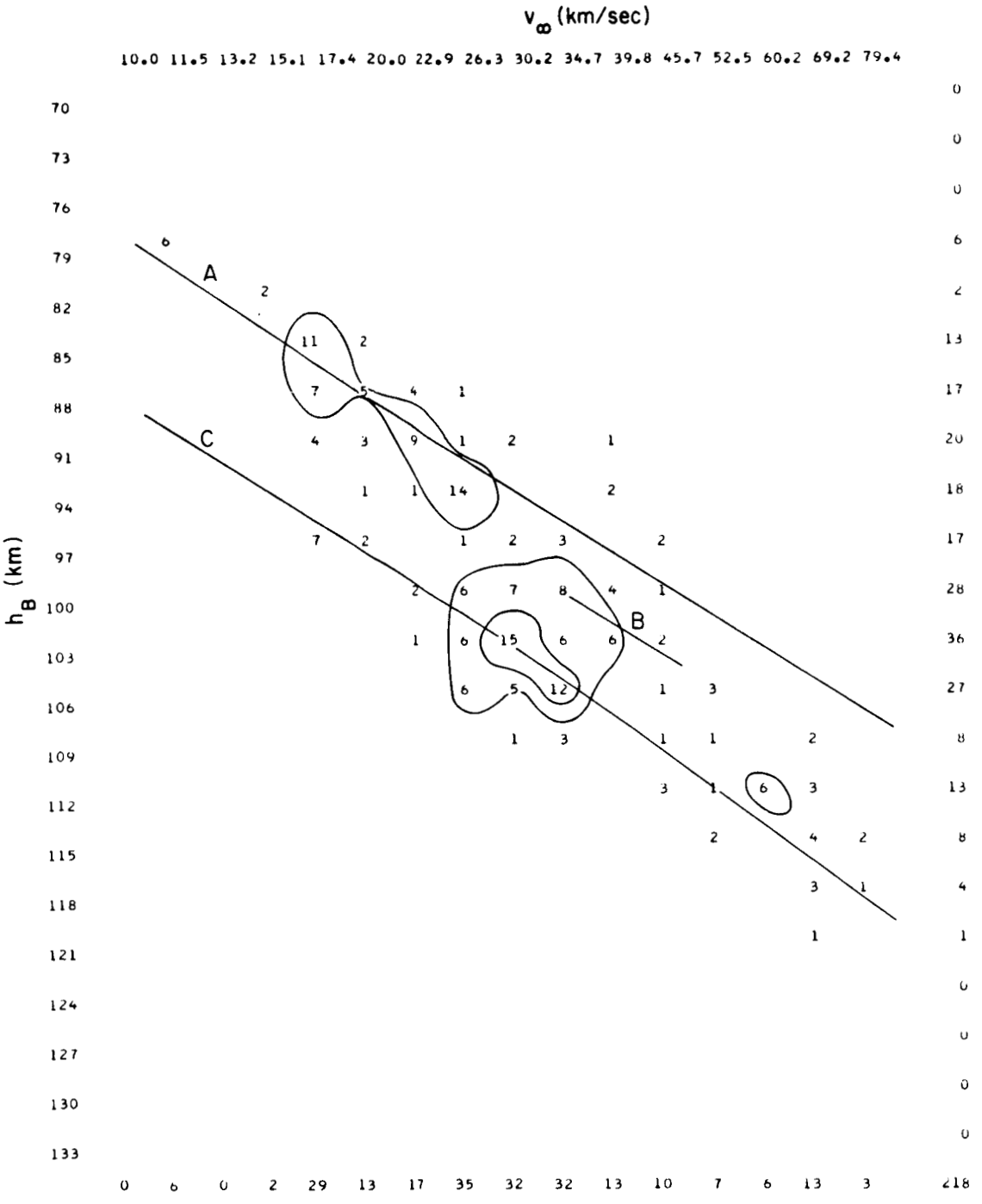

Figure 18. The same as Figure 17, but for $0 \leq \log m_{ph}/m_d < 0.8$. The C_1 group is the most pronounced, the C_2 group starts to form, the A and B groups are weaker than in Figure 17. (Jacchia's meteors with $\cos Z_R \geq 0.5$.)

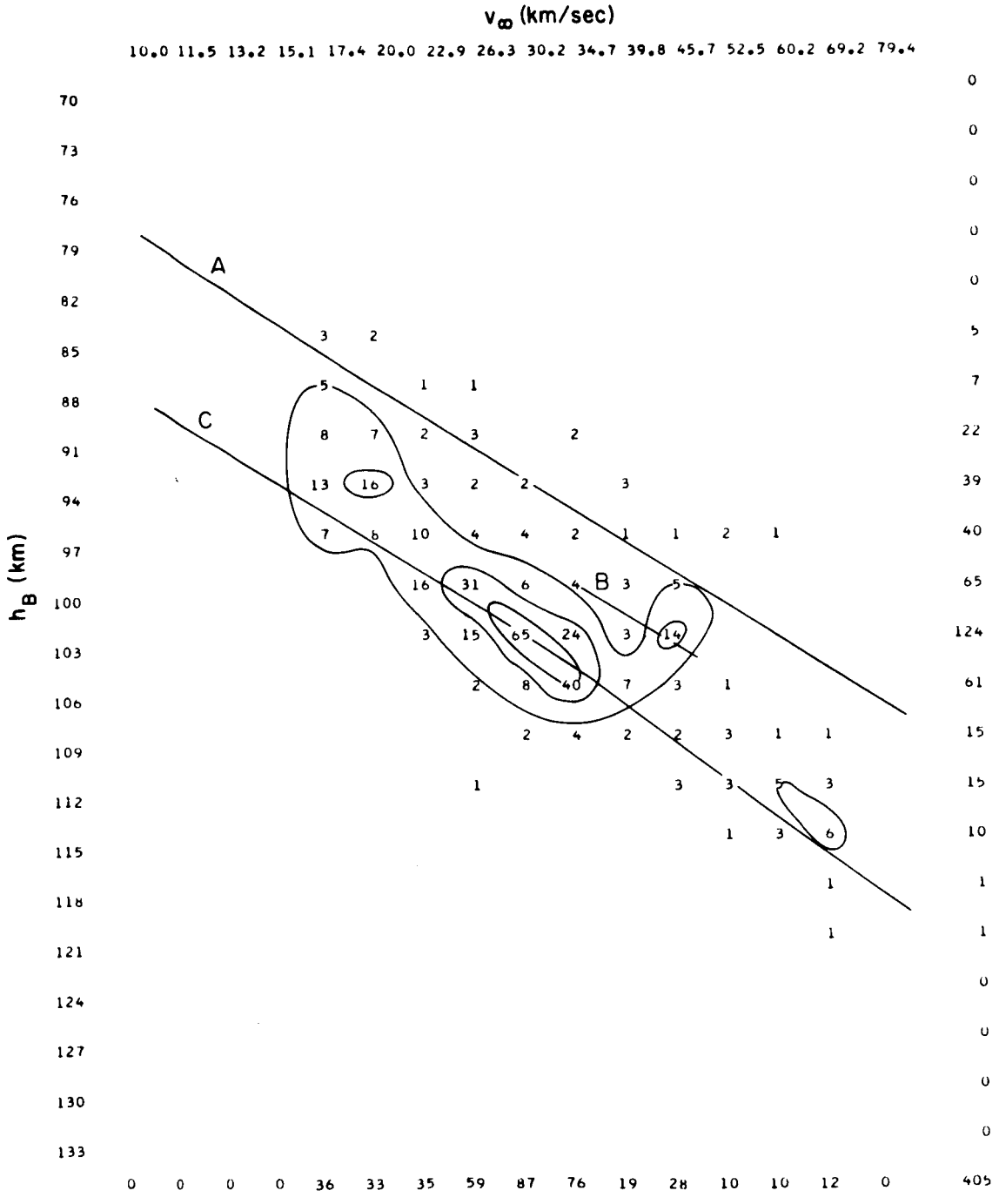

Figure 19. The same as Figure 17, but for $0.8 \leq \log m < 1.5$. The C_1 group is only slightly contaminated by the A and B groups. (Jacchia's meteors with $\cos Z_R \geq 0.5$.)

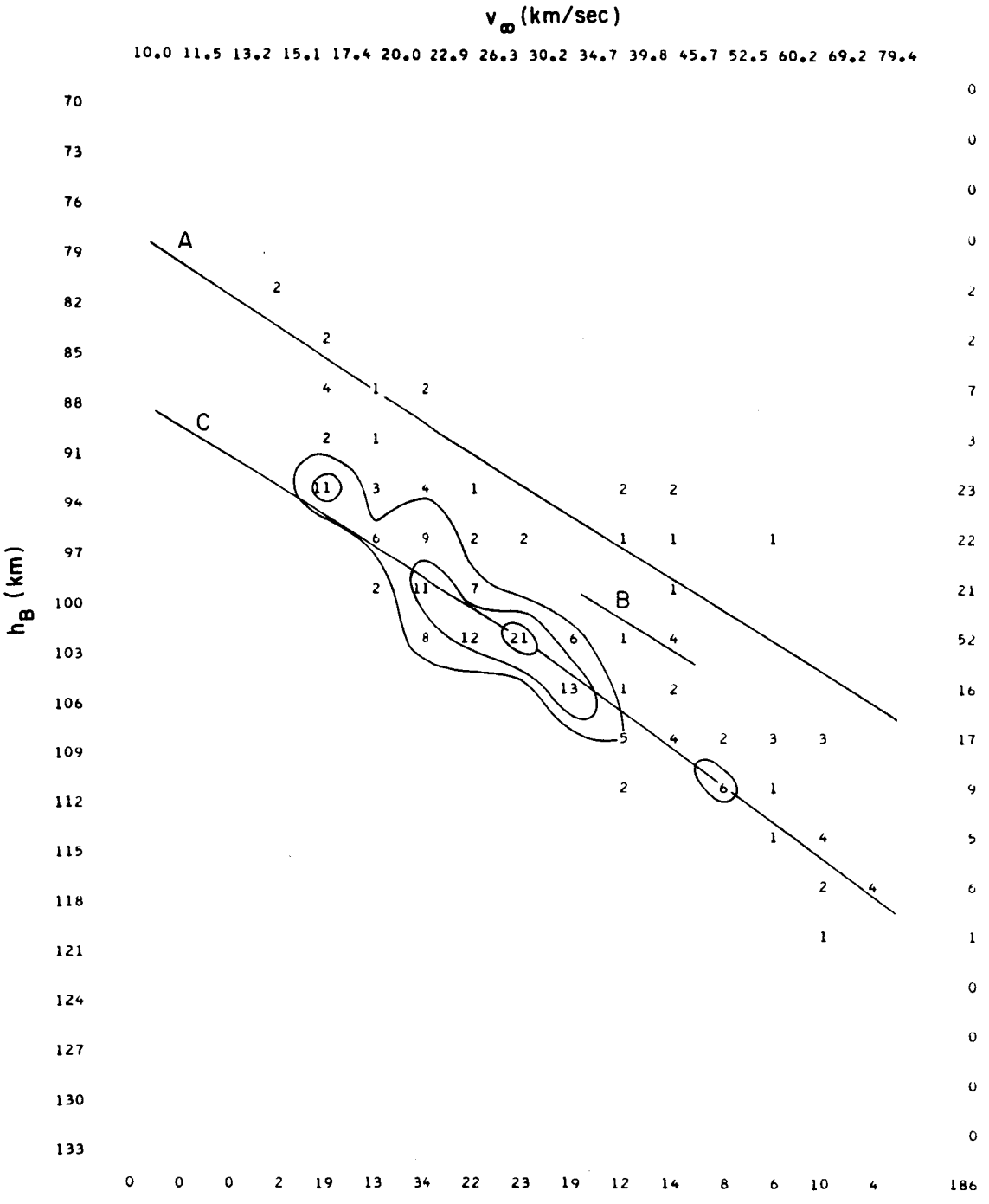

Figure 20. The same as Figure 17 but for $1.5 \leq \log m_{ph}/m_d < 3$. The C_1 and C_2 groups are the only ones present. (Jacchia's meteors with $\cos Z_R \geq 0.5$.)

2.9 Beginning Heights of Iron-Meteor Particles

There is not very much observational material for any definitive conclusion. As pointed out by McCrosky (1968), there is no guarantee that pure iron meteor spectra are really connected with solid-iron meteoroids. If one examines the results of all experiments with artificial meteoroids, the spread of beginning height is almost 30 km, which might be explained by some serious preheating of the meteoroid surface due to the shape charge explosion. When the first two experiments were performed (McCrosky and Soberman, 1963; McCrosky, 1968), the preheating was expected to be small. The observed beginning heights were 6 and 3 km lower than the A level. The corresponding values for the two meteors with iron spectra are 7 km and 9 km (Ceplecha, 1967). Because of the spread, one could simply deduce that the iron bodies have beginning heights lower than the A level.

2.10 Bright Meteors and Fireballs

We must be very cautious in the study of the beginning heights of these bright objects; small-camera meteors are statistically inhomogeneous, owing to the larger dynamic range of meteor magnitudes, and observational material from observatories throughout the world must be combined (Ceplecha, 1967). The situation is even worse if we use results of the Prairie Network cameras (McCrosky, 1967, private communication), where the dynamic range of meteor magnitudes is even larger and the sensitivity of the cameras is low. The distance of meteors from the Prairie Network stations is also unfavorable to beginning-height studies.

Nevertheless, we can recognize the same levels in the h_B-v_∞ plots for small-camera meteors as were found for Super-Schmidt meteors. The A group is less significant than in the case of the McCrosky-Posen Super-Schmidt meteors. All three groups have approximately the same number of meteors, which means the C group as a whole is stronger than the A group.

The Prairie Network meteors are not suitable for beginning-height studies: the spread of magnitudes is too wide, and the observed pattern could mostly be due to observational effects connected with the geometrical conditions of visibility. One fact is of course almost certain: The C_2 group is virtually absent (McCrosky, 1967). Thus, it seems that the bright Super-Schmidt meteors and the small-camera meteors have a preponderance of strong C_2 groups. The sporadic faint meteors and fireballs have only an insignificant number of the C_2-group meteors with high velocity.

The maximum of the distribution of the ratio of photometric and dynamic mass for Prairie Network meteors is systematically shifted by about 2 orders relative to the same distribution for Super-Schmidt meteors. The main maximum for Prairie Network meteors is almost at the place previously found for the Super-Schmidt-meteor A-group maximum (Ceplecha, 1966). The least-squares solution for exponents in the drag equation, where the dynamic mass was replaced by the photometric mass (Ceplecha, 1966), gave all three exponents (X, Y, Z) values close to 2.2 instead of the theoretical value 3. This is much closer to the single-body theory than in the case of Super-Schmidt meteors. If the least-squares solution is obtained for the group of Prairie Network meteors with lowest beginning heights, all three exponents are quite close to 3, the value of the single-body theory.

2.11 Shower Meteors

We have so far dealt mainly with sporadic meteors. Figure 21 (the h_B-v_∞ plot) illustrates the position of each meteor shower as given by Jacchia et al. (1967). The lines of the -2.5 and -3.5 velocity exponents are given at exactly the same positions as plotted in Figure 16. On the whole, the showers are close to the C level. The Draconids are the well-known exception, and they begin 7 km higher than the average C level; but this is still somewhat closer to the C level than the distance of the A level from the C level. The C_1 group is found for α Capricornids, κ Cygnids, Southern Taurids, Northern Taurids; the C_2 group for Lyrids, σ Hydrids, Perseids, and Orionids; the B group for Geminids, δ Aquarids, ι Aquarids, and Quadrantids. There is no case of a connection between any classical shower

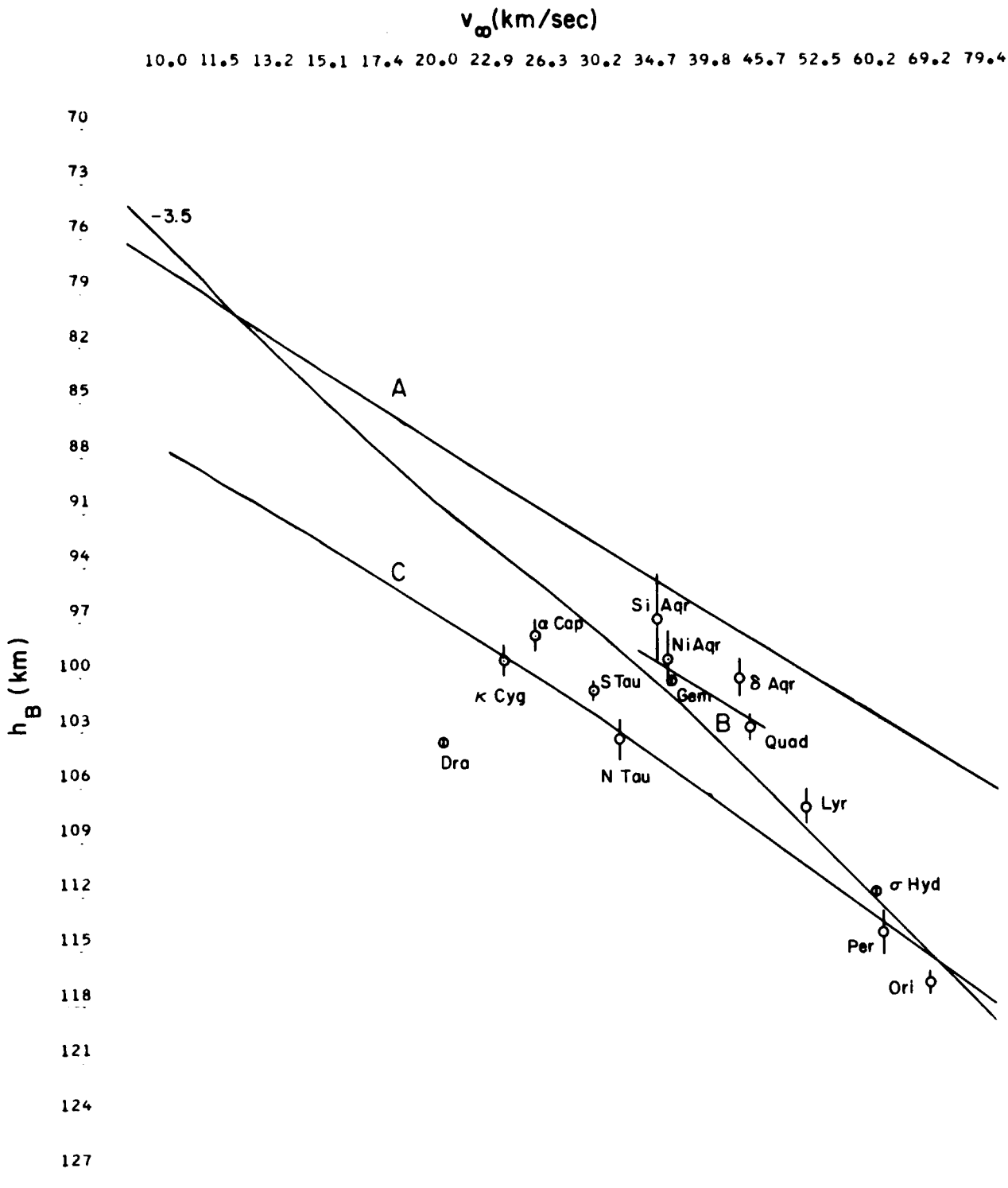

Figure 21. Positions of individual showers in the h_B-v_∞ plot. The A, B, and C levels of the -2.5 velocity exponent are the same as in Figure 16. Jacchia's shower meteors are used. The -3.5 velocity exponent level is given for comparison.

and the A level. The orbital characteristics of the above-mentioned showers are the same as those of sporadic meteors at the same positions in Figure 21. The Quadrantids are the only exception; they form the only shower with beginning heights at B level and with large perihelion distances. With the exception of Draconids and Quadrantids, there is no difference in principle between the shower meteors and the sporadic meteors belonging to the B and C levels.

2.12 End Heights and Lengths

Figure 22 represents the number of meteors in the end-height initial-velocity (h_E-v_∞) plots, where the McCrosky-Posen meteors are used. The two main levels found for beginning height are not distinct for the end heights, indicating that longer luminous trajectories are characteristic for the C level. The two lines plotted in Figure 22 represent the A and C levels. They were simply derived from the plot in Figure 1 by computing the average end heights along the A and C lines and then represented in Figure 22. Thus, the average end-height difference between A and C groups seems to be 5 km and to increase slightly with velocity. The broad distribution of h_E for each velocity interval in Figure 22 is partly caused by the masking effect of cos Z_R (cos $Z_R \geq 0.5$ in Figure 22) on the separation of the two maxima of the A and C levels, which is smaller than in the case of beginning heights. The velocity exponents, n, for the end heights ($\rho_B \propto v_\infty^{-n}$) are: A group, between 1 and 2 with an average of 1.4; C_1 group between 1 and 2 with an average value of 1.5; C_2 group, between 3 and 4 with an average value of 3.6. The complete picture in Figure 22, without separating the groups according to Figure 1, could be represented by a velocity exponent of about 2, which is consistent with the value found by Jacchia et al. (1967). The comparison of beginning and end heights for the A and C levels is plotted in Figure 27.

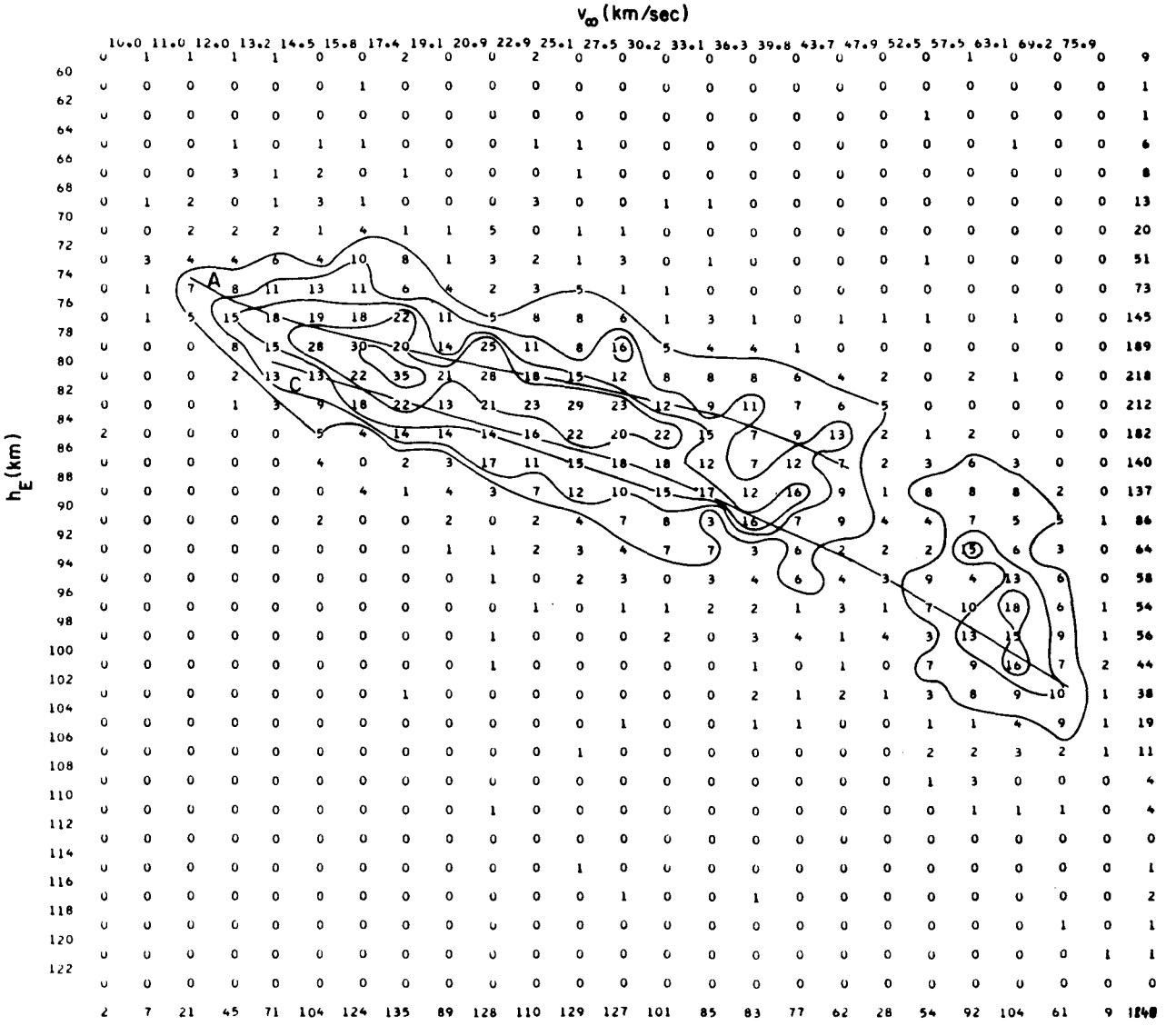

Figure 22. This is a complete analogy of Figure 1, but the end heights are used instead of beginning heights. Thus, the numbers of McCrosky-Posen sporadic meteors with $\cos Z_R \geq 0.5$ inside two-dimensional intervals of h_E-v_∞ are given. The two main levels are much closer in the h_E-v_∞, and the statistical spread makes just one broad maximum between them.

Figure 22 indicates that meteor length could be important for the study of beginning-height groups. If we plot the average length of sporadic meteors with $\cos Z_R \geq 0.5$ as it changes along the -2.5 lines of the A and C levels of Figure 1, we get Figure 23. The A group has extremely short trajectories, almost half those of C_1-group meteors with the same velocity. The B group is intermediate between A and C_1. An important fact is that the C_2 group is clearly separated from the C_1 group by short trajectory lengths. This is caused mainly by differences in the $\cos Z_R$. The inclination of the orbit was previously used to separate C_1 from C_2 (Ceplecha, 1967). Figure 23 shows that the length of the meteor luminous trajectory could be used to distinguish between C_1 and C_2 groups. The separation of the A from the C level by meteor length is represented in Figures 24 and 25, where the numbers of meteors in the h_B-v_∞ plot are used. If we consider the statistical spread of the approximately reduced McCrosky-Posen meteors, we clearly see the separation of the A group (mainly with $\ell \leq 12$ km) from the C group (mainly with $\ell < 12$ km).

There is a systematic change of $\cos Z_R$ with velocity along the lines of individual groups (Figure 26). The $\cos Z_R$ value for the A group is generally close to 0.8. For the C level it decreases from 0.90 to 0.75 inside the C_1 group, and suddenly changes to 0.90 again when entering the C_2 group. For the C_2 group, it decreases again from 0.90 to 0.75. The average beginning heights are compared with the average end heights in Figure 27.

2.13 Summary of Observational Results

1. Beginning heights of photographic meteors have two main levels inclined approximately by -2.5 in the h_B-v_∞ plot. These two levels exist together, at least in the velocity interval from 20 to 40 km sec^{-1}, and are separated by an approximately 10-km difference in the beginning height. I will refer to the lower level as the A level and to the corresponding meteors as the A group; the higher level will be the C level and the corresponding meteors the C group.*

*This notation is consistent with my previous papers.

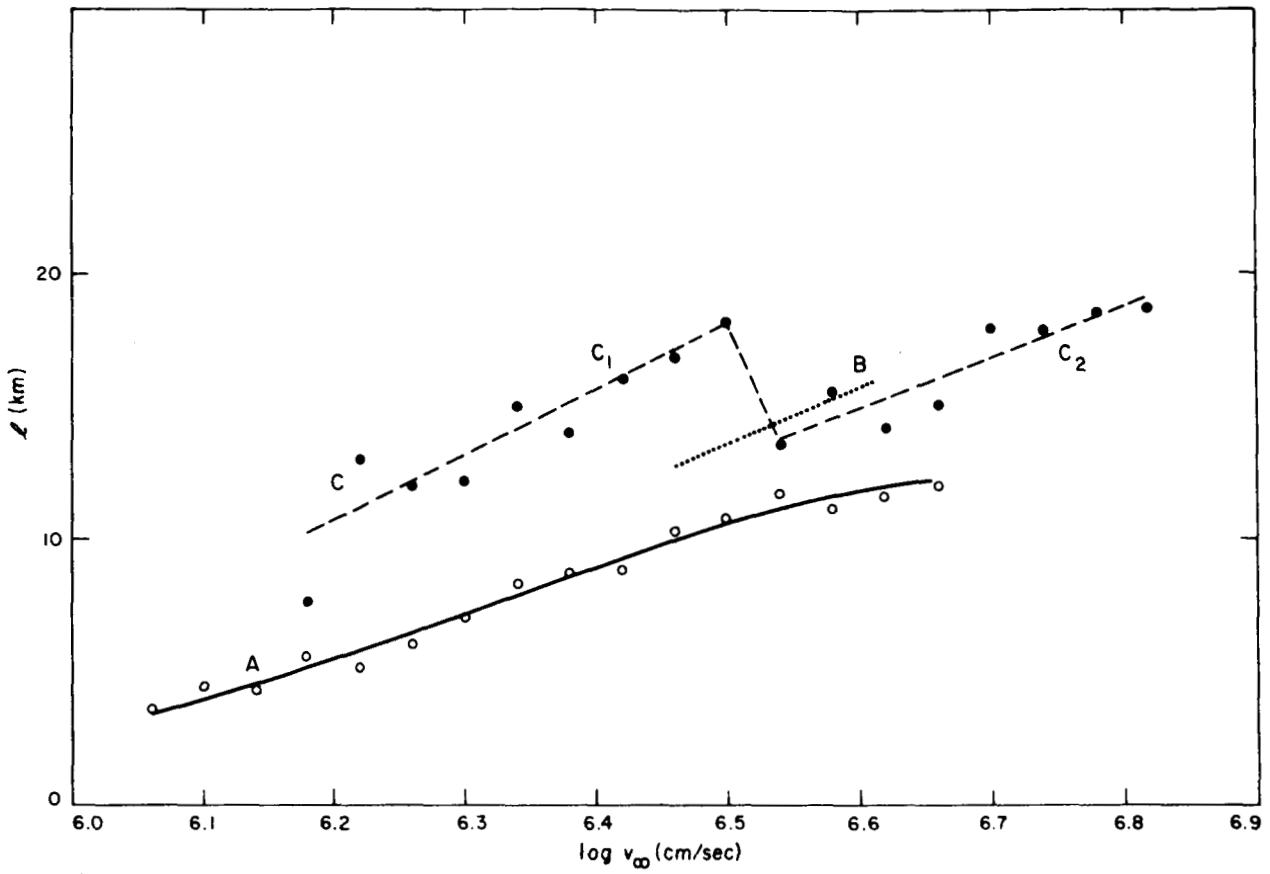

Figure 23. The average lengths of luminous trajectories computed along the A, B, and C lines of Figure 1 are plotted against log v_∞. The A group has much shorter orbits than the C group. The C_2 group has shorter orbits than the C_1 group, mainly because of geometrical conditions (cos Z_R). (McCrosky-Posen sporadic meteors with cos $Z_R \geq 0.5$.)

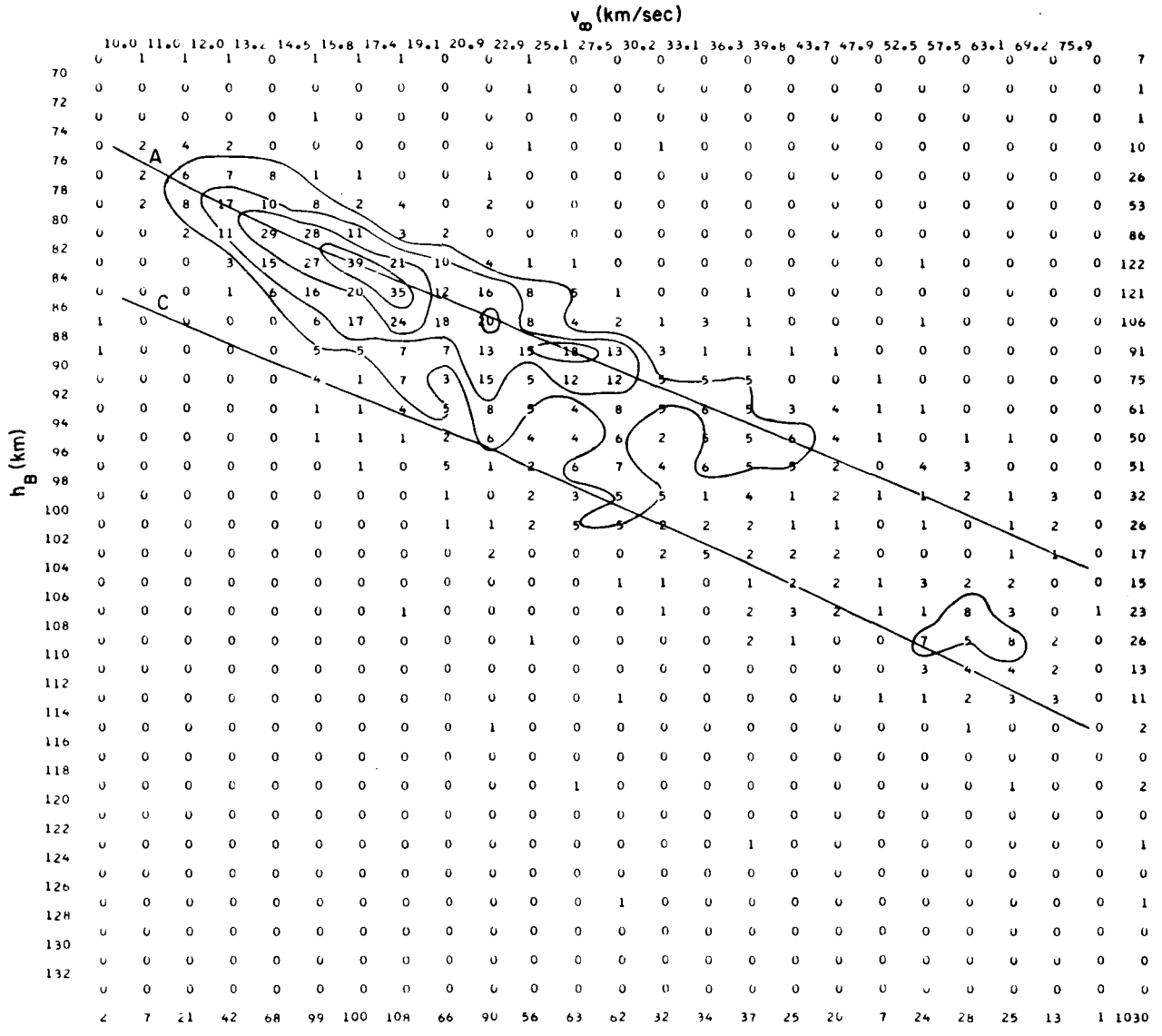

Figure 24. McCrosky-Posen sporadic meteors with cos $Z_R \geq 0.5$ and with the length of the luminous trajectory ≤ 12 km are given in the same plot as Figure 1. The A and C levels are those of Figure 1. The A group is predominant.

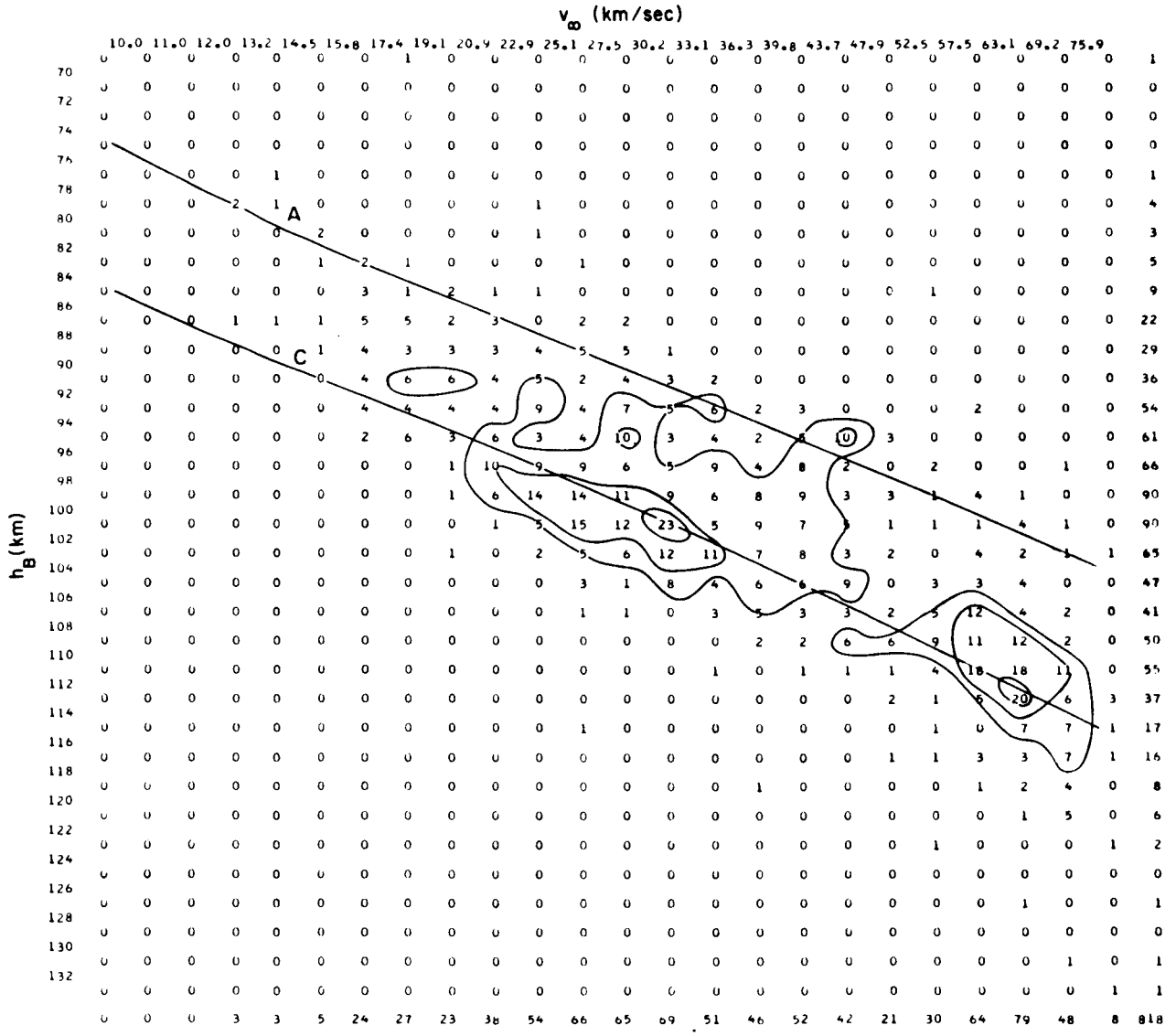

Figure 25. The same as Figure 24, but with length of the luminous trajectory greater than 12 km. The C_1 and C_2 groups are predominant. (McCrosky-Posen sporadic meteors with $\cos Z_R \geq 0.5$.)

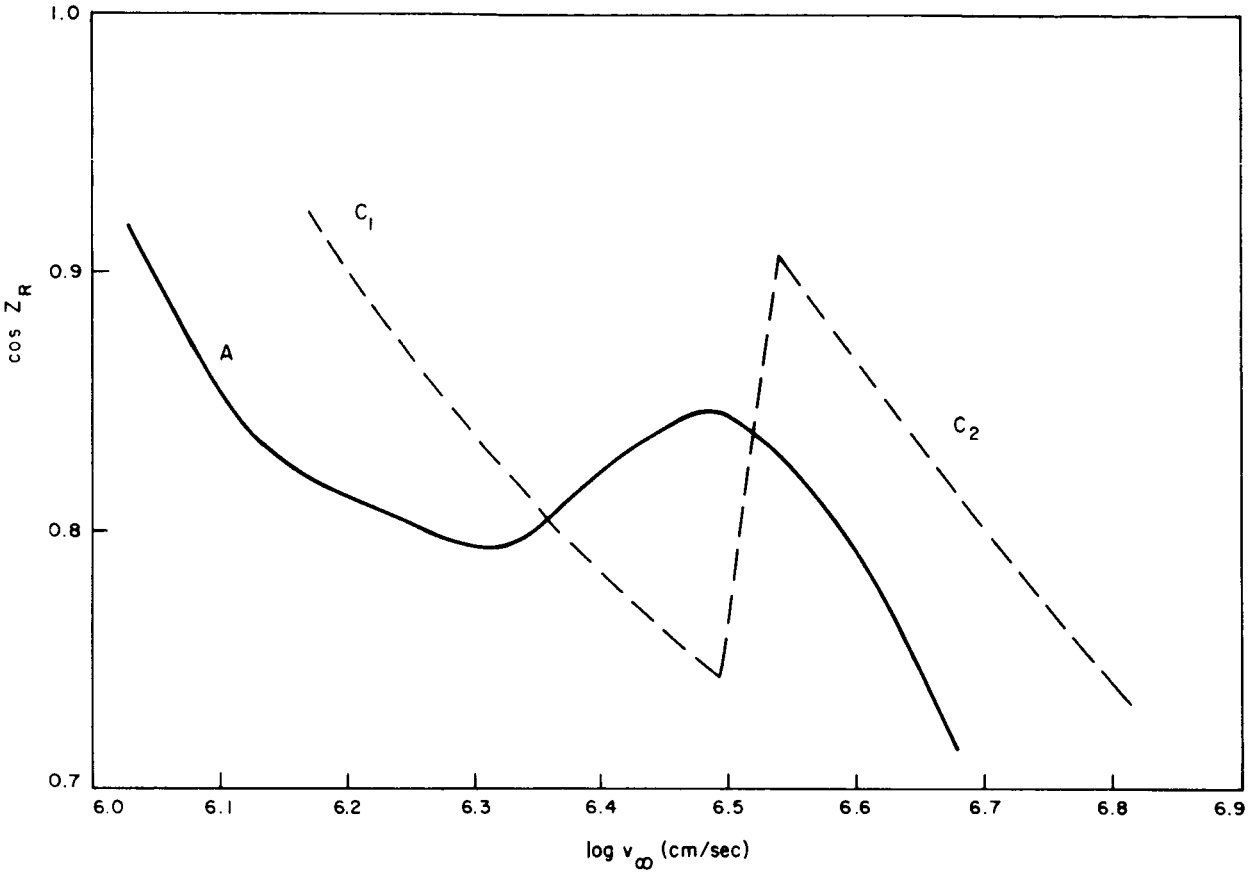

Figure 26. Average cos Z_R was computed along the A and C levels of Figure 1 and plotted against the log v_∞. The difference of lengths between the C_1 and C_2 groups is shown to be due to the difference of average cos Z_R. (McCrosky-Posen sporadic meteors with cos $Z_R \geq 0.5$.)

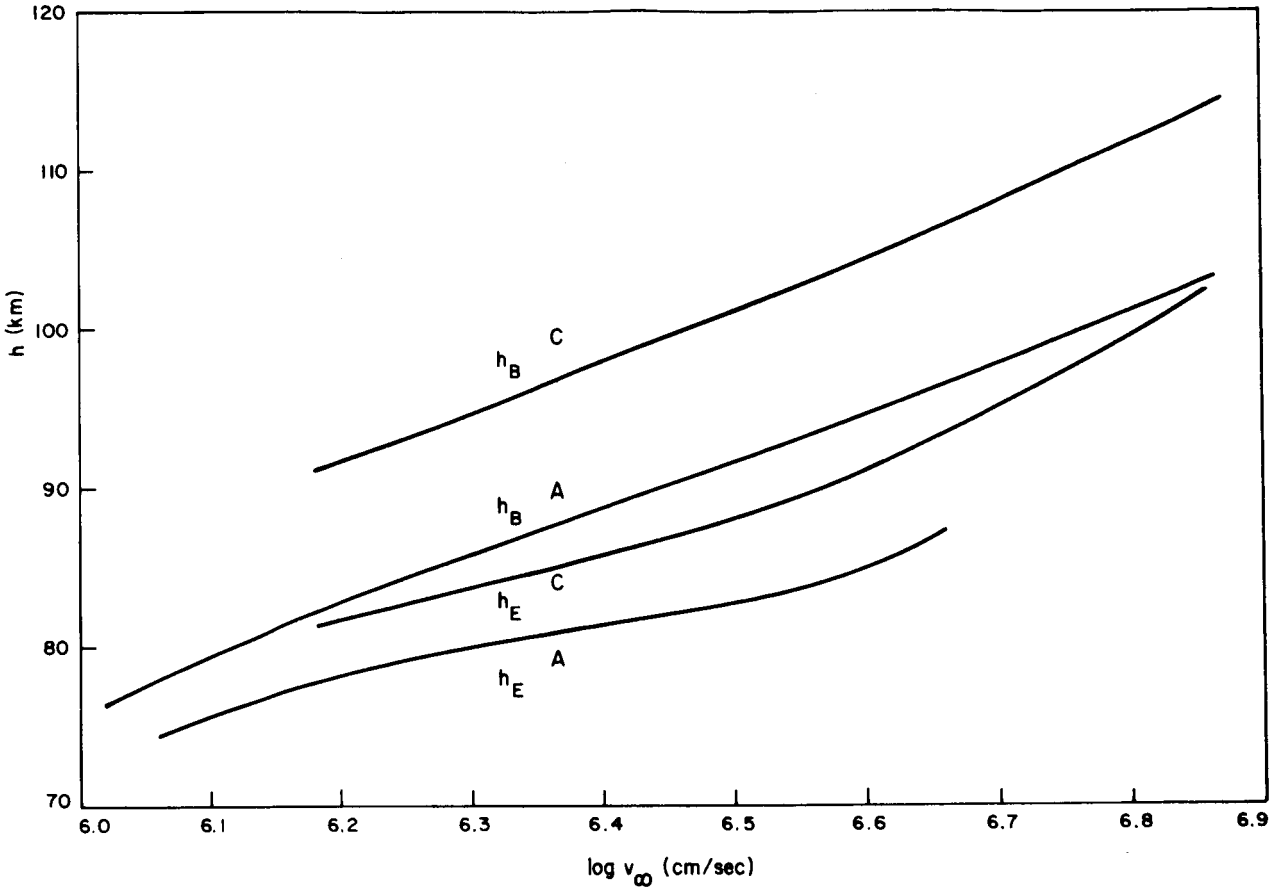

Figure 27. A synopsis of the average beginning and end heights for the A and C levels is given in the same plot. The beginning heights of the A group are close to the end heights of the C level. (McCrosky-Posen sporadic meteors with $\cos Z_R \geq 0.5$.)

2. The C group of meteors shows two maxima of distribution with velocity. The maximum close to 30 km sec^{-1} is connected with ecliptically concentrated orbits, and I will call it the C_1 group. The maximum close to 60 km sec^{-1} is connected with random inclinations of the orbits, and I will refer to it as the C_2 group.

3. The orbits of the A and C_1 groups have aphelion distances less than 6 a.u., and their orbital planes have inclinations less than 40°. The orbits of the C_2 group have aphelion distances greater than 6 a.u. and are randomly inclined. Thus, the criterion of 6 a.u. cannot separate the A from the C_1 group.

4. Meteors with $q < 0.25$ define an intermediate level (which I will call B group) in the h_B-v_∞ plot between 30 and 50 km sec^{-1}.

5. The differences in orbital elements between the A and C_1 groups cannot be explained by differences in the velocity.

6. The C_2 group is more pronounced for meteors with brightness from 1 to about -6 mag. The relative number of short-period and less-eccentric orbits belonging to the A group increases with decreasing brightness of Super-Schmidt meteors. Meteors with $v_\infty < 15$ km sec^{-1} belong only to the A group. The C level is not observed at these low velocities.

7. The average end heights of the A-group meteors are about 5 km lower than those of the C-group meteors. The end-height levels for the A and C_1 groups are inclined by approximately -1.5 in the ρ_E - v_∞ plot; the C_2 level is inclined by -3.6 in the same plot.

8. If the velocity dependence is removed, the shortest luminous trajectories belong to the A group and the longest to the C_1 group; the C_2 group has shorter luminous trajectories than the C_1 group.

9. There is a systematic change of cos Z_R with velocity along the A and C levels and a sudden change from the C_1 to the C_2 group.

10. The C level is connected with the 1- to 2-order ratio of the photometric and the dynamic mass. The A level is connected with meteors for which the difference between the photometric and the dynamic mass is small.

11. The separation between A and C groups is not connected with daily and seasonal variations. An actual index of magnetic activity measured at Tucson shows no relation to the separation of beginning height of Super-Schmidt meteors into two main A and C levels.

12. The classical meteor showers do not differ from the sporadic meteors of the B and C groups. The only exceptions are the γ Draconids with beginning height 7 km higher than the C group at the same velocity. This means that they differ by almost the same (slightly less) height interval from the C level as the C level differs from the A level at the same velocity.

13. Meteors with pure iron spectra and artificial iron meteoroids have beginning heights lower than the A group at the same velocity. The difference is not greater than 10 km.

3. INTERPRETATION

3.1 Possible Explanations

I consider that there are the following possible explanations for the above observational facts:

1. meteoroid composition,
2. fragmentation and spraying,
3. additional radiation of an abnormal nature at the beginning (different from the normal radiation by emission lines of metals),
4. variation of air density in the 90- to 100-km heights,
5. change of the aerodynamic flow regime,
6. difference in the meteor surface temperature at the beginning height,
7. rotation.

Interpretation 4 is partially answered by the observational fact 11. If variations of air density are responsible for the two beginning-height levels, then these variations ought to be different from the daily, seasonal, and magnetic-index variations. This seems highly improbable as an explanation for the total effect, which could be explained only by changes of air density by a factor of 5 to 6.

If one examines explanation 3, the forbidden oxygen line could be a possibility because it started to emit light some 10 km higher than the main meteor radiation. But the "blue" emulsion used for the Super-Schmidt cameras is not sensitive at this particular wavelength. Thus, a similar "air radiation" in the blue spectral region must be a matter for conjecture. Nothing of this nature is known at the present time, but the spectral distribution of meteor light is not known for the brightness interval of Super-Schmidt meteors. There is, of course, the contrary indication that the faint meteors do radiate relatively more in the red region.

Explanation 6 is closely connected with the composition and structure of the body. One cannot imagine any reason why two identical bodies reached the conditions for sufficient ablation with surface temperatures at the ratio of 6 to 1.

Explanation 7 means that the A level must be connected with sufficiently rotating meteoroids and the C level with nonrotating meteoroids. This is equivalent to a 4 to 1 input ratio of heat on the surfaces. This ratio is roughly consistent with the height difference of the A and C levels; but if one considers all the orbital differences between A and C, then this explanation also fails.

A different heat transfer coefficient Λ at greater heights has a direct influence on the beginning height. Thus, the two beginning-height levels, A and C, could be explained by two different values of Λ, which could correspond to two different aerodynamic-flow regimes. The coexistence of these two levels in the velocity interval from from 20 to 40 km sec^{-1} of course nullifies this explanation as being the only one. It means the meteors at these levels must differ in dimensions at the same velocity. The composition or fragmentation must be accepted together with the change of flow regime to explain the coexistence of A and C levels in this broad velocity interval.

If one assumes that the Super-Schmidt meteors are so small that radiation cooling starts to be decisive at the beginning height, then the only explanations of the two levels could be: differences in rotation, heat transfer, or emmissivity.

Hence, the observational results must be explained mainly by interpretations 1 or 2.

3.2 Meteoroid Composition

Meteoroid composition was proposed as the only explanation in my earlier paper (1967), where "composition" is understood to be represented by the product of heat capacity, thermal conductivity, and bulk density of a body.

The observational evidence presented in Section 2.13 is more complex than in that paper: thus, some revision seems to be necessary. If one still wished to use only meteoroid composition to explain the two levels of beginning height, then the following facts are favorable.

If the composition-density relationship suggested earlier (Ceplecha, 1967) is valid, then observational fact 1 requires density of the A-group meteors to be 3 times greater than that of the C group meteors, which seems reasonable. The end-height difference mentioned in 7 is also consistent with this density ratio. It is evident from 2 that C_1 and C_2 have the same composition. The lack of the C group with $v_\infty < 15$ km sec^{-1} mentioned in 6 could be explained simply by the nonexistence of bodies with correspondingly short-period orbits within the C group. Thus, a possible explanation of observational fact 12 is that the C group is connected with the cometary system, which, together with observational fact 3, means that the C_1 group is connected with short-period comets and the C_2 group with long-period comets.

The existence of the γ Draconids could be explained by their extremely low bulk density, which should be 2 or 3 times less than the average density of the C group. Observational fact 13 means that the absolute bulk density is lower for the meteors of the A and C groups than for iron. The bulk density of the A-group meteors is then between 7.7 and 2.5 g cm^{-3}, for the C group between 2.5 and 0.8 g cm^{-3}, and for the γ Draconids between 0.3 and 0.8 g cm^{-3}. These densities are consistent with observational fact 10.

The difference in the velocity exponents at the end heights for the C_1 and C_2 groups (observational fact 7), as well as observational fact 8, could not be explained by the composition. But both these, according to 9 could be explained by some geometrical effect due to the differences between the conditions of collision of meteoroids with the earth in long- and short-period orbits.

There is really no direct observational evidence to disprove the meteoroid-composition explanation.

3.3 Fragmentation and Spraying

Fragmentation could be important in explaining the two main levels (A and C) of beginning height if it takes place before the beginning point. Then the A level could be that of a single body and the C level that of fragments or droplets. This means that the C level is one of radiation cooling and the A level of heat-conductivity cooling (Ceplecha and Padevět, 1961). The difference in height of these two levels is about right, but the velocity exponent for the C group ought to be 3. The 2.5 exponent is not surprising, however, if we consider that a part of the heat-conductivity height is contained in fragments, which is simply due to a "reference height" where the fragments were separated from the main body (and heat conductivity is the only possible process for energy output at this height for meteors of Super-Schmidt dimensions).

The absence of the C group with $v_\infty < 15$ km sec^{-1} is evidence that fragmentation is an explanation. Any small fragment with such a velocity is decelerated so strongly that the temperature could not reach that for vaporization. Thus, only the single-body level is expected at these velocities, and $v_\infty < 15$ km sec^{-1} corresponds to the dimensions of stony fragments less than about 70 μ in radius. This is consistent with a recent paper by Simonenko (1967) and two earlier papers by Smith (1954) and McCrosky (1968).

Spraying, instead of fragmentation, is probably impossible owing to the fact that the height interval from the melting point to vaporization is substantially smaller than the difference between the A and C groups. The spray starts too late to enable it to produce the C level; the spray level is probably lower than the C level.

One fact detracts from the explanation of fragmentation as the only cause of the observed A and C levels of beginning height: fragmentation should start much higher than the C level. The temperature on the surface of the meteoroid at that time is quite low and the structure of the body would be

extremely fragile. But the A level (interpreted in this chapter as the single-body level), according to 13, corresponds to densities of the body of at least 2.5 g cm^{-3}, which could hardly be fragile enough. Also, the existence of of γ Draconids is not consistent with this interpretation: the height level for evaporation of small fragments with radiation cooling could not be so high, or the single fragments must have very low densities. The existence of an intermediate B group is also not quite consistent with this interpretation. On the other hand, there is good agreement with observational facts 7, 8, and 10. It seems that the explanation by fragmentation only is less probable than the explanation by composition.

3.4 Meteor Densities

Even if we assume that the A and C levels of beginning height can be explained by fragmentation, the average density of the A group would be at least 2.5 g cm^{-3}. Hence, the C group does not reflect any difference in composition but does reflect a difference between the dimensions of fragments and those of the body belonging to the A level.

If we explain the A and C levels as two different composition groups of meteors, we get the average bulk densities of the A group in a broad interval with resemblance to the stony meteorite densities, and the average bulk densities of the C group somewhere close to 1. If we also consider the orbital elements of the meteors of each particular group, we are inclined to explain the C group as comets (C_1 connected with short-period comets, and C_2 with long-period comets), and the A group as meteoroids with densities similar to the meteorite densities (Ceplecha, 1967). I intentionally omitted the term "asteroidal" since the origin of A-group meteoroids is a completely different problem from that of their average bulk densities.

Verniani (1965) computed the meteoroid bulk densities using luminous and drag equations, which are assumed to be valid during the light trajectory of the meteor. This is completely different from the present paper, where I use the meteor trajectory before the light begins. Verniani equated dynamic

and photometric masses and thus attributed all the differences in these masses to the difference in bulk density. For the same observational material, I computed (1966) the least-squares solution for the exponents in the equations used by Verniani. The computed exponents are completely different from the theoretical ones used by Verniani. Since the theoretical equations are not consistent with the observational material, any value of the average bulk density computed with theoretical exponents will probably be in error. Observational fact 10 of this paper and my previous results (1966) favor acceptance of the meteorite densities for the A group of meteors, and densities somewhere close to 1 for the C group. There are so many discrepancies in our present knowledge of meteors that no final conclusions on the bulk densities of meteors should be drawn either from the beginning heights or from the comparison of photometric and dynamic mass.

The difference between the dynamic and photometric masses may be, in great part, caused by the nonvalidity of the simple equations of meteor physics. The conventional luminous equation and the drag equation, as they are applied to the measurement of the meteor image, may contain the flaw.

4. ACKNOWLEDGMENT

I am very much indebted to Dr. R. E. McCrosky for discussing many of the problems reviewed in this report and permitting me to use his unpublished material on the Prairie Network fireballs. My special thanks are due to Miss M. Ježková for preparing numerical computations for the MINSK-22 computer at the Ondřejov Observatory, and to Mrs. A. Posen for preparing the programs for the CDC-6400 computer at the Smithsonian Astrophysical Observatory. I am grateful to Dr. L. G. Jacchia for his careful reading and criticism of my manuscript.

5. REFERENCES

CEPLECHA, Z.

1958. On the composition of meteors. Bull. Astron. Inst. Czechoslovakia, vol. 9, pp. 154-159.

1966. Dynamic and photometric mass of meteors. Bull. Astron. Inst. Czechoslovakia, vol. 17, pp. 347-354.

1967. Classification of meteor orbits. Smithsonian Contr. Astrophys., vol. 11, pp. 35-60.

CEPLECHA, Z. and PADEVĚT, V.

1961. The beginning of rapid evaporation of meteors of different dimensions. Bull. Astron. Inst. Czechoslovakia, vol. 12, pp. 191-195.

JACCHIA, L. G.

1958. On two parameters used in the physical theory of meteors. Smithsonian Contr. Astrophys., vol. 2, no. 9, pp. 181-187.

1960. Individual characteristics of meteor families (abstract). Astron. Journ., vol. 65, pp. 53-54.

JACCHIA, L. G., VERNIANI, F. and BRIGGS, R. E.

1967. An analysis of the atmospheric trajectories of 413 precisely reduced photographic meteors. Smithsonian Contr. Astrophys., vol. 10, no. 1, pp. 1-139.

McCROSKY, R. E.

1958. The meteor wake. Astron. Journ., vol. 63, pp. 97-106.

1967. Orbits of photographic meteors. Smithsonian Astrophys. Obs. Spec. Rep. No. 252, 20 pp.

1968. Meteors without sodium. Smithsonian Astrophys. Obs. Spec. Rep. No. 270, 16 pp.

McCROSKY, R. E. and POSEN, A.

1961. Orbital elements of photographic meteors. Smithsonian Contr. Astrophys., vol. 4, no. 2, pp. 15-84.

McCROSKY, R. E. and SOBERMAN, R. K.

1963. Results from an artificial iron meteoroid at 10 km/sec. Smithsonian Contr. Astrophys., vol. 7, pp. 199-208.

SIMONENKO, A. N.

1967. Dimensions of particles escaping from meteor bodies during flares. Comets and Meteors, vol. 2, no. 15, pp. 34-44.

SMITH, H. J.

1954. The physical theory of meteors. V. The masses of meteor-flare fragments. Astrophys. Journ., vol. 119, pp. 438-442.

U.S. STANDARD ATMOSPHERE

1962. U.S. Standard Atmosphere 1962. Prepared under NASA, USAF, and USWB, Washington, D. C., 278 pp.

VERNIANI, F.

1965. On the luminous efficiency of meteors. Smithsonian Contr. Astrophys., vol. 8, no. 5, pp. 141-172.

1967a. Comments on Ceplecha's paper "Classification of meteor orbits." Smithsonian Contr. Astrophys., vol. 11, pp. 61-63.

1967b. Further comments by F. Verniani. Smithsonian Contr. Astrophys., vol. 11, p. 65.

BIOGRAPHICAL NOTE

ZDENĚK CEPLECHA received the RNDr. degree from Charles University, Czechoslovakia, in 1952 and the C. Sc. and D. Sc. degrees from the Czechoslovak Academy of Sciences in 1955 and 1967, respectively.

Since 1951 Dr. Ceplecha has been an astrophysicist with the Astronomical Institute of the Czechoslovak Academy of Sciences in Ondřejov. In 1968 he held a National Research Council Postdoctoral Visiting Research Associateship at the Smithsonian Astrophysical Observatory.

Dr. Ceplecha's principal field of investigation is meteors and meteoroids.

NOTICE

This series of Special Reports was instituted under the supervision of Dr. F. L. Whipple, Director of the Astrophysical Observatory of the Smithsonian Institution, shortly after the launching of the first artificial earth satellite on October 4, 1957. Contributions come from the Staff of the Observatory.

First issued to ensure the immediate dissemination of data for satellite tracking, the reports have continued to provide a rapid distribution of catalogs of satellite observations, orbital information, and preliminary results of data analyses prior to formal publication in the appropriate journals. The Reports are also used extensively for the rapid publication of preliminary or special results in other fields of astrophysics.

The Reports are regularly distributed to all institutions participating in the U. S. space research program and to individual scientists who request them from the Publications Division, Distribution Section, Smithsonian Astrophysical Observatory, Cambridge, Massachusetts 02138.